# NOISE AND VIBRATION ANALYSIS OF A DRUM BRAKE USED IN HEAVY COMMERCIAL TRUCKS

**A Thesis Submitted to**
**the Graduate School of Engineering and Sciences of**
**İzmir Institute of Technology**
**in Partial Fulfillment of the Requirements for the Degree of**

**MASTER OF SCIENCE**

**in Mechanical Engineering**

**by**
**Osman AKDAĞ**

**May 2018**
**İZMİR**

We approve the thesis of **Osman AKDAĞ**

**Examining Committee Members:**

**Prof. Dr. Bülent YARDIMOĞLU**
Department of Mechanical Engineering, İzmir Institute of Technology

**Prof. Dr. Serhan ÖZDEMİR**
Department of Mechanical Engineering, İzmir Institute of Technology

**Prof. Dr. Hasan ÖZTÜRK**
Department of Mechanical Engineering, Dokuz Eylül University

**09 May 2018**

**Prof. Dr. Bülent YARDIMOĞLU**
Supervisor, Department of Mechanical Engineering,
İzmir Institute of Technology

**Prof. Dr. Metin TANOĞLU**
Head of the Department of
Mechanical Engineering

**Prof. Dr. Aysun SOFUOĞLU**
Dean of the Graduate School
of Engineering and Sciences

# ACKNOWLEDGEMENTS

I would like to express my deepest graduate to my advisor, Prof. Dr. Bülent YARDIMOGLU because of his chair, gumption and spiritual support during my thesis. And also Prof. Dr. YARDIMOGLU has an open office door, it is free to organize a meeting to find answer all question in graduated and under graduated education.

I am truthfully obligated to my family for their trust and support during my life.

In addition to these, I really appreciate family of Ege Fren for their knowledge and information for this study.

# ABSTRACT


## NOISE AND VIBRATION ANALYSIS OF A DRUM BRAKE USED IN HEAVY COMMERCIAL TRUCKS

Heavy commercial duty vehicles have been used to for many years. High energy dissipation is required to stop these types of vehicles. Selection of brake type is related with the brake resists to this physical and environment conditions and also comfortability of drivers and passengers. Brake squeal is the most common costumer complaint for brake systems. This problem is main interest and tackled in many ways.

In this thesis, vibration characteristics of the heavy commercial duty brake system, which is a drum brake, is studied by Finite Element Method to analyze the brake squeal. Natural frequencies and mode shapes of drum and shoe which are in frictional contact are determined by using ANSYS. Block Lanczos solver is preferred for this analysis.

Experimental modal tests are accomplished to compare finite element results with experimental ones. Then, the noise characteristics of the brake system are obtained by performing a series dynamometer tests. In these experiments, four parameters are selected to investigate the decreasing and eliminating the noise. The selected parameters are deceleration rate, pressure, temperature and friction coefficients. The results are presented in tables and graphs.

# ÖZET

## AĞIR TICARI KAMYONLARDA KULLANILAN KAMPANA FRENLERIN SES VE TITREŞIM ANALIZLERI

Ağır ticari görev araçları uzun yıllardan beri kullanılmaktadır. Bu tür araçları durdurmak için yüksek enerji dağılımı gereklidir. Fren tipinin seçimi, frenin bu fiziksel ve çevre koşullarına; ayrıca sürücü ve yolcuların konforu ile ilgilidir. Fren sistemleri için fren çığlığı en yaygın müşteri şikayetidir. Bu sorun ana ilgi konusudur ve birçok yönden ele alınmaktadır.

Bu tez çalışmasında, tamburlu freni olan ağır ticari fren sisteminin titreşim karakteristikleri, fren çığlığını incelemek için Sonlu Elemanlar Yöntemi ile çalışılmıştır. Sürtünmeli temasta olan tambur ve balataların doğal frekansları ve titreşim şekilleri ANSYS kullanılarak belirlenmştir. Bu analiz için Block Lanczos çözücü tercih edilmiştir.

Sonlu eleman sonuçlarını deneysel olanlarla karşılaştırmak için deneysel modal testler gerçekleştirilmiştir. Ardından, fren sisteminin gürültü karakteristikleri bir dizi dynamometer testi yapılarak elde edilmiştir. Bu deneylerde, gürültüyü azaltmak ve ortadan kaldırmak için dört parametre seçilmiştir. Seçilen parametreler yavaşlama hızı, basınç, sıcaklık ve sürtünme katsayılarıdır. Elde edilen sonuçlar tablo ve grafiklerde sunulmuştur.

# TABLE OF CONTENTS

# LIST OF FIGURES

# LIST OF TABLES

# LIST OF SYMBOLS

| | |
|---|---|
| $a_i$ | fourier coefficient |
| $A$ | accelerance matrix |
| $b_i$ | fourier coefficient |
| $c_i$ | damping coefficient |
| $f$ | force vector |
| $F_i$ | frictional forces |
| $F_1$ | reaction force acting piston due to shaft |
| $F_2$ | reaction force acting from piston to shoe |
| $F_3$ | reaction force acting from piston to trailing shoe |
| $F_4$ | reaction force acting from piston to leading shoe |
| $F_7$ | reaction force acting from abutment to trailing shoe |
| $F_8$ | reaction force acting from abutment to leading shoe |
| $k_i$ | spring stiffness |
| $k_j$ | stiffness of contact |
| $K$ | stiffness coefficient |
| $m$ | mass coefficient |
| $M$ | mass coefficient |
| $M_i$ | normal forces of shoes |
| $M_{in}$ | shaft moment |
| $N_i$ | normal forces of drum and shoe |
| $x$ | displacement vector |
| $X$ | displacement amplitude vector |
| $Y$ | mobility matrix |
| $Z$ | dynamic stiffness matrix |
| | |
| $\alpha$ | proportionality constant of damping |
| $[\alpha]$ | matrix form of frequency response function |
| $\beta$ | proportionality constant of damping |
| $\theta_i$ | location of pressure center |
| $\omega$ | vibration frequency |

# CHAPTER 1

# GENERAL INTRODUCTION

In automotive industry, several types of brakes such as drum or disc brakes have been used since first vehicle. At the beginning, the drum brakes were most popular. However, in the last years, the disc brakes are used more than another one. Lots of different parts are used in assemble of vehicles. Because of that reason, all geometrical parameters of parts such as dimensions and tolerances are important for assemble. On the other hand, some parts of vehicles are considered as safety components. One of the safety parts of vehicle is brake. Also, comfortability of vehicle is critical for human healths. Therefore, all the afromentioned constraints should be taken into account in designing phase of vehicle components. Although all these issues are known, costumer complaints can be arised. One of these complaints is related with brake squeal.

Types of brake squeals are given in Figure 1.1. Brake squeals are treated in two groups as high frequency squeal and low frequency squeal. Low frequency squeal has frequency under 3 kHz, otherwise it is known as high frequency squeal. Low frequency brake squeal is related with suspension, knuckle and brake parts. However, high frequency is related with rotor and pads of brake. The noise generated by drum or brake disc are based on friction forces during braking.

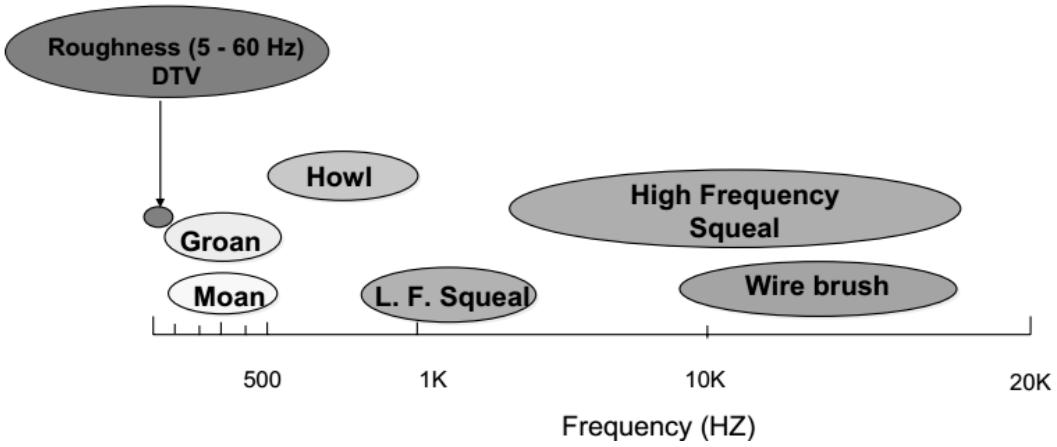


Figure 1.1. Types of brake squeal
(Source: Liu, 2002)

## 1.1. Literature Review

Spurr (1961) reported that conditions of linings are the main reason for drum brake squeal. He mentioned also that the temperature difference in linings during its operations especially after a series of usage in frequently. Thus, he concluded that brake squeal often occurs when the brake system is cooled itself after heavy-duty stops.

Okamura and Nishiwaki (1989) improved an analytical model for brake squeal based on kinetic energy. They obtained that kinetic energy increment in one cycle is related with the coupled vibration of radial and tangential directions of drum. Also, they added that friction coefficient, fixing of brake shoe, location of lining on shoe are important on brake squeal.

Nishiwaki (1993) stated the brake noise classification. According to his classification, if the frequencies fall into the range of 1-15 kHz, the noise is called brake squeal and if they are in the range of 200-500 Hz, it is called as brake groan noise. He outlined that both noise is generated by the brake system due to variations of friction forces.

Day and Kim (1996) presented finite element modal analysis for drum brake with S-cam shaft, shown in Figure 1.2, used in heavy commercial vehicle for noise problem. They analyzed the stiffness of contact and components which are effective on natural frequencies and drum asymmetry. They proposed that the drum asymmetry is more effective than stiffness of parts or contacts.

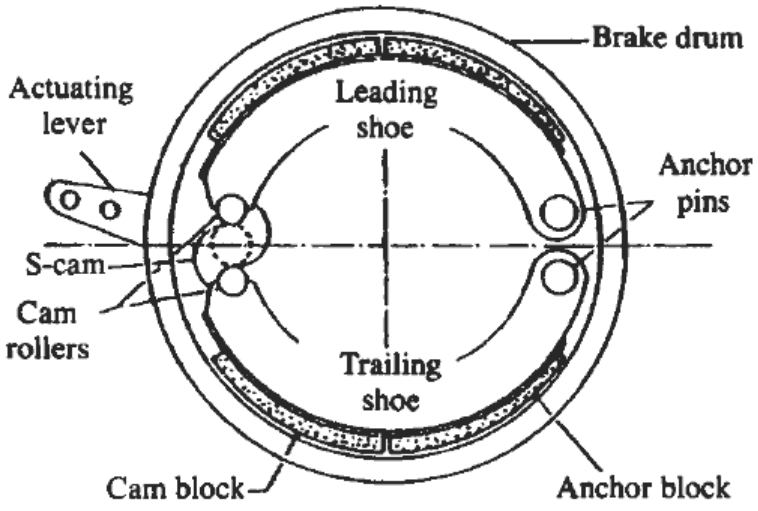


Figure 1.2. S-cam Drum brake
(Source: Day and Kim, 1996)

Lee et al (2001) carried out a theoretical study for a drum brake having non-uniform cross-sectioned shoes, shown in Figure 1.3, to investigate the drum brake squeal. They found that if the cross-sectional area of shoe increases while it's bending stiffness decreasing, the drum brake squeal reduces.

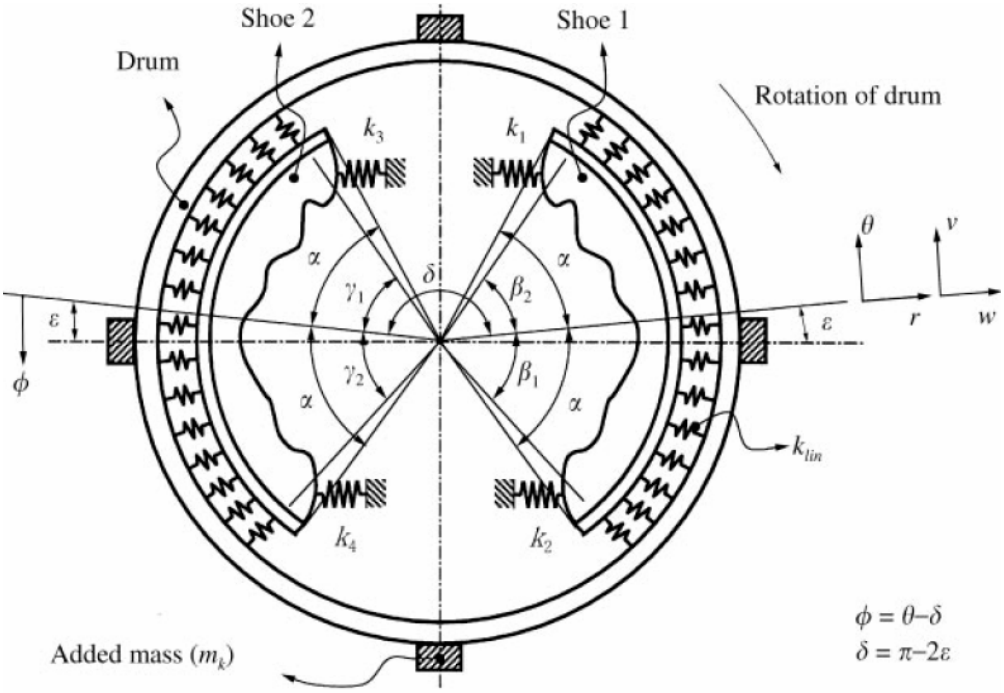


Figure 1.3. Model of drum brake with non-uniform cross-sectioned shoes
(Source: Lee et al, 2001)

Somnay and Shih (2002) presented a method to predict heavy vehicle drum brake squeal by using finite element model. They tuned the dynamic characteristics of their numerical model by comparing their experimental test results. Their finite element model have contact interface for the lining and drum to simulate the frictional behaviour so that it gives asymmetric stiffness matrix. Therefore, they focused on dynamic characteristics such as the frequency and damping which is related with stability for non noisy system.

Zhou et al (2007) developed the five degrees of freedom non-linear model for vibration of a drum brake. They focused on low frequencies.

Hussin et al (2010) investigated the worning of lining effect on drum brake squeal. They reported that dynamic properties of the lining are changed due to the braking in its normal operations. They performed modal testing for new and worn linings. Also, they carried out squeal tests by using brake dynamometer and measured squeal frequencies up to 10 kHz. They outlined the results as follows:

- Natural frequencies of new and worn lining are slightly different,
- Modal coupling is potentially a reason for the squeal,
- Althougth the new and worn linings has positive and negative dampings, respectively, theoretical results for new ones or not in agreement with the experimental results. Therefore, negative damping is not main reason of squeal,
- Enviromental conditions of lining material such as temperature, humidity and physical parameters such as pressure, drum speed, and friction coefficients are effective on both types of linings,
- When the humidity has the values in the interval 60% to 80%, new and worn lining propagate a squeal.

Glisovic et al (2010) studied experimentally the effect of friction coefficient on drum brake squeal at low frequencies. They emphasized that the effects such as temperature, humidity, velocity, and pressure are important for selecting of lining material.

Ahmed et al (2012) analyzed the reasons for drum brake squeal by finite element methods. They modeled the structure, as shown in Figure 1.4, in ANSYS to determine the instability for drum brake by considering the prestresses. Similar to model of Somnay and Shih (2002), they have unsymmetric stiffness matrix due to the same reason. They showed that the contact stiffness between drum and lining is important for brake squeal. Additionaly, they stated that the brake squeal is proportional to friction coefficient between drum and lining. Moreover, they noted that squeals generally arise if the modal characteristics of drum and shoes are near to the coupled vibration frequency.

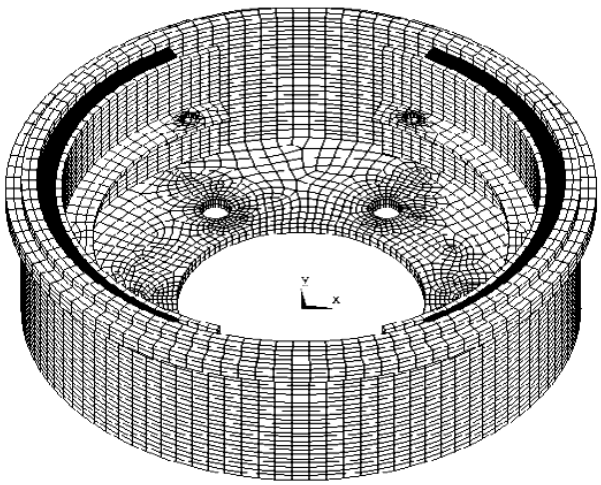

Figure 1.4. FEA model (modified)
(Source: Ahmet et al, 2012)

Teoh et all (2013) developed a two degrees of freedom model shown in Figure 1.5 in order to analyze the drum brake squeal. It can be seen from Figure 1.5 that the excitation of the system is based on the frictional interaction of drum and lining. They carried out transient analysis of the developed theoretical model under braking forces and found 2026 Hz for brake squeal frequency. They also verified their theoretical model by their experimental study of which set up is shown in Figure 1.6. Their measured frequency was 1950 Hz. Therefore, the percentage difference between theoretical and experimental values is about 4%. Studies with increased damping and decreased contact stiffness under the friction coefficient in the range of 0.1-0.5 were treated as positive to eliminate the squeal. Furthermore, it is noted that low relative velocity due to high friction coefficient can excite the large amplitude of vibration and also sliding velocity has a critical value proportional to braking load.

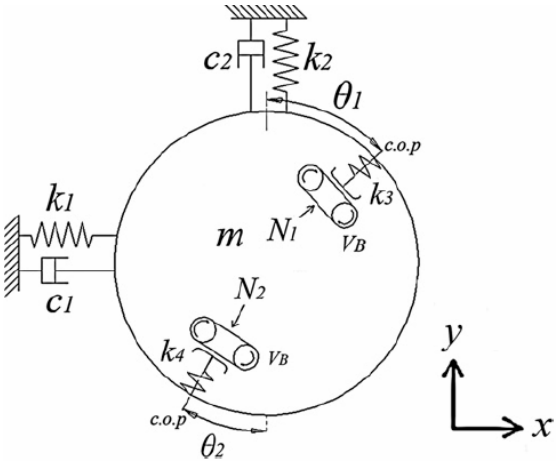


Figure 1.5. Drum brake model
(Source: Teoh et al, 2013)

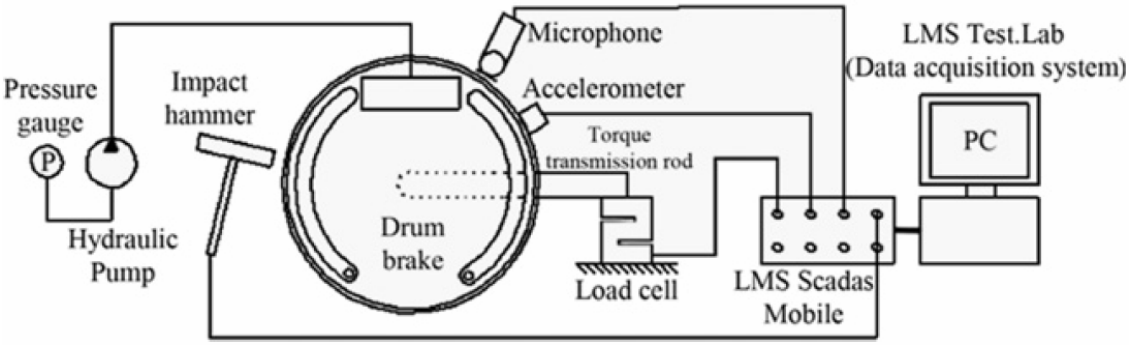


Figure 1.6. Test setup for drum brake squeal
(Source: Teoh et all, 2013)

Phatak and Kulkarni (2017) presented a drum brake noise problem solution in passenger cars by using finite element vibration analysis. They found that brake spider is critical for noise reduction. They shifted the natural frequency from 2283 Hz to 1893 Hz by modifying the geometries of the spider as shown in Figure 1.7.

Actual design of brake shield

Modified design of brake shield

Figure 1.7. Modification of brake shield (modified)
(Source: Phatak, 2017)

## 1.2. Objectives of Study

Objective of this study is to obtain vibration and noise characteristics of the heavy commercial duty brake system shown in Figure 1.8. Also, it is intended to eleminate or to reduce noise. More specific goals of this research can be listed as follows:

- to obtain free vibration characteristic of non-simplified drum and shoe by using finite element method,
- to find natural frequencies of the assembled system having drum and shoe with frictional interaction
- to present parametric studies of vibration analysis by using finite element method,
- to determine the noise characteristics of the whole brake in dynamometer tests,
- to validate numerical results with experimental ones.

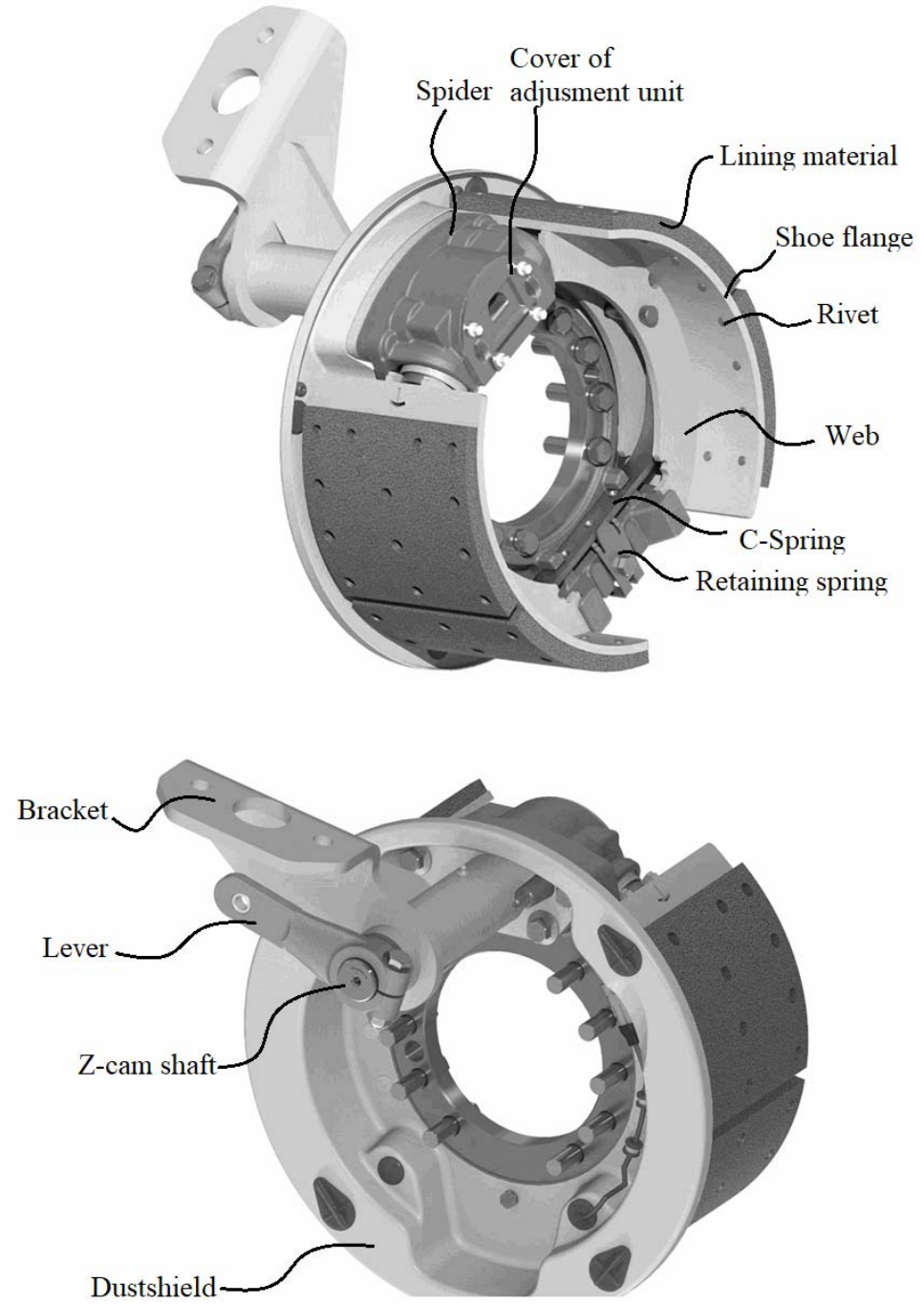


Figure 1.8. Z-cam drum brakes

# CHAPTER 2

# THEORETICAL BACKGROUND

## 2.1. Geometrical Background of Drum Brakes

For the heavy commercial vehicles, two types of brakes such as drum and disc brakes are used. Disc brakes are common for road vehicle and construction series on Europe. In Turkey and Asian countries, drum brakes are used for construstion vehicle. There are several drum brake types such as cam brake, wedged brake, simplex brake, and duplex brakes as shown in Figure 2.1. Cam brakes are also in two types as S-cam and Z-cam drum brakes. Another grouping of drum brakes is based on shoe assembles and type. In this case, single leading, twin leading, leading trailing combination etc. can be said.

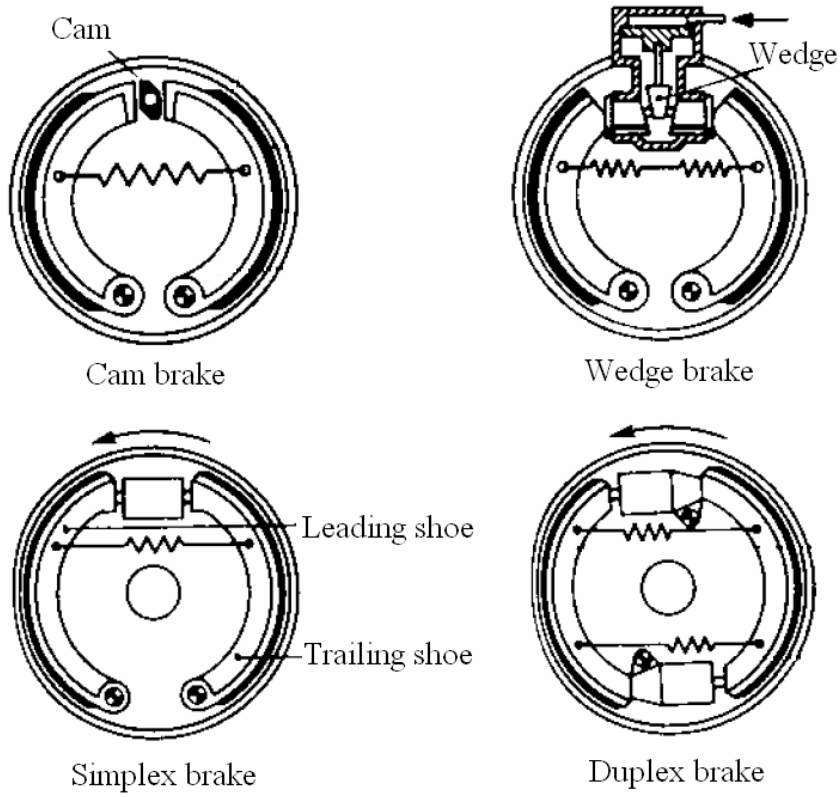


Figure 2.1. Types of drum brakes
(Source: Orthwein, 2004)

## 2.2. Forces acting on Z-Cam Drum Brake

Free body diagram of Z-cam drum brake is shown in Figure 2.2. Input moment $M_{in}$ is provided by a lever connected to shaft. In ajduster unit, there are two pims used to transfer the torque from shaft to piston as force. Then, the pistons push the shoes and braking is occured.

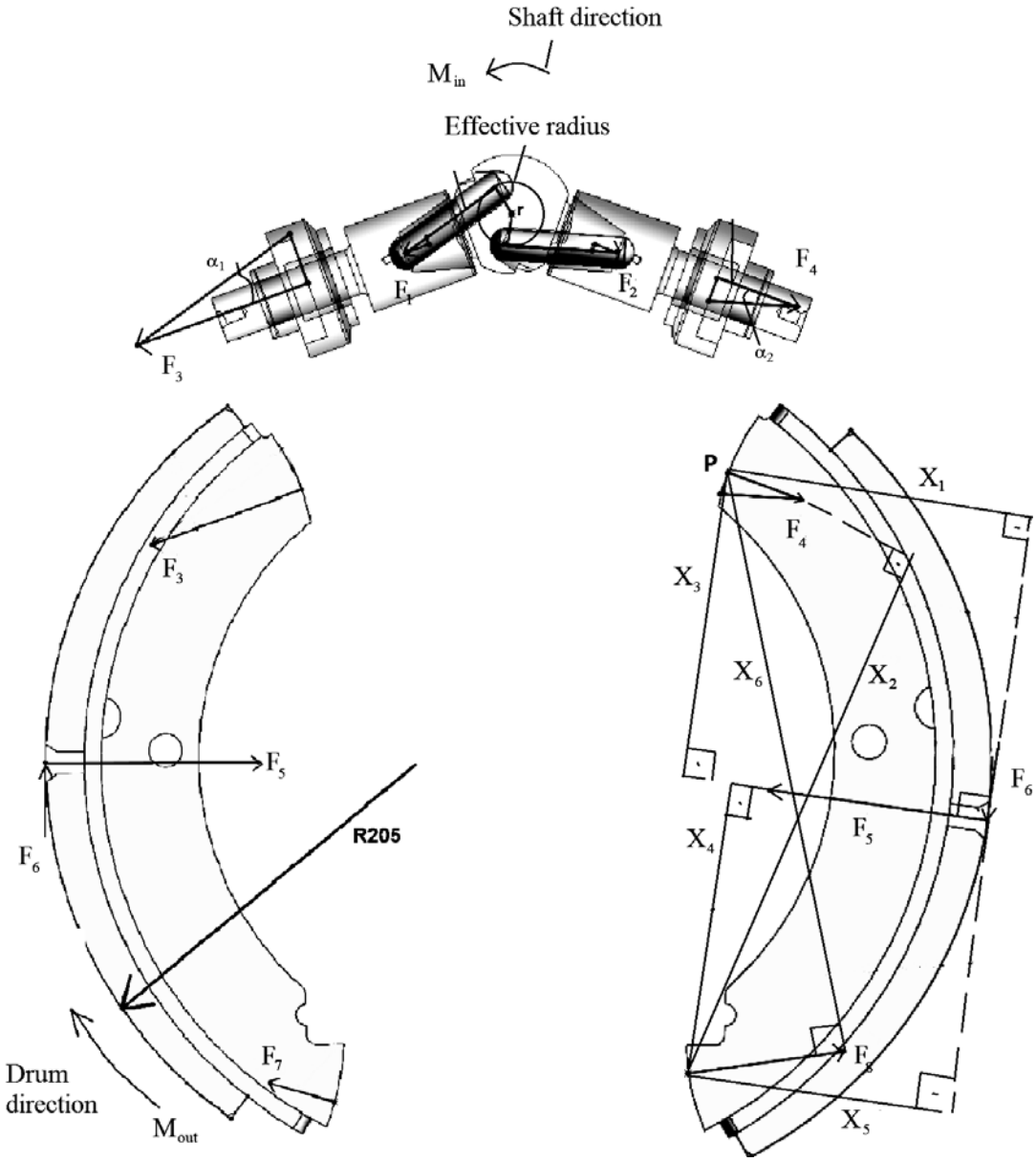


Figure 2.2. Free body diagram of Z-cam drum brake

$M_{in}$ is the shaft moment in counterclockwise direction. $F_1$ and $F_2$ are the reaction forces acting on pins due to shaft. Directions of these forces are tangent to effective radius $r$ of Z-cam. As seen from the free body diagram shown in Figure 2.2, the shoes have input

forces $F_3$ and $F_4$. Moreover, shoes are under frictional force $F_6$ due to normal force $F_5$ and reaction forces of abutment end $F_7$ and $F_8$. Starting from $M_{in}$, all forces can be found by using equilibrium equations.

## 2.3. Eqution of Motion for Drum Brakes

As a simple example for equation of motion for drum brake, the model given by Teoh et all (2013) is selected to present here. The brake model having two degree of freedom is shown in Figure 2.3.

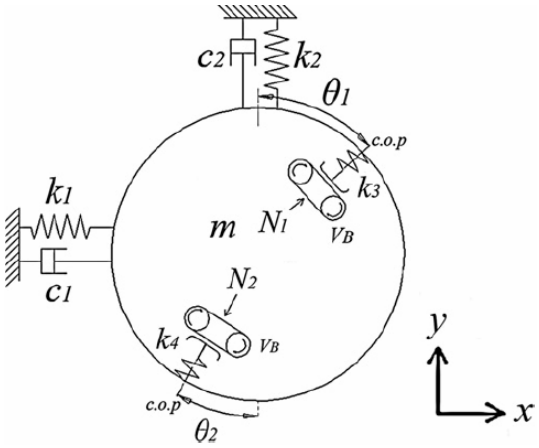


Figure 2.3. Drum brake model
(Source: Teoh et al, 2013)

The equation of motion for the model shown in Figure 2.3 is given by Teoh et all (2013) as

$$\begin{bmatrix} m & 0 \\ 0 & m \end{bmatrix} \begin{Bmatrix} \ddot{x} \\ \ddot{y} \end{Bmatrix} + \begin{bmatrix} c_1 & 0 \\ 0 & c_2 \end{bmatrix} \begin{Bmatrix} \dot{x} \\ \dot{y} \end{Bmatrix} + \begin{bmatrix} k_{11} & k_{12} \\ k_{21} & k_{22} \end{bmatrix} \begin{Bmatrix} x \\ y \end{Bmatrix} = \begin{Bmatrix} F_1 \\ F_2 \end{Bmatrix} \tag{2.1}$$

where

$$k_{11} = k_1 + k_3 \sin^2 \theta_1 + k_4 \sin^2 \theta_2 \tag{2.2}$$

$$\begin{aligned} k_{12} = {} & k_3 \sin \theta_1 \cos \theta_1 + k_4 \sin \theta_2 \cos \theta_2 \\ & \pm \mu_0 k_3 \cos^2 \theta_1 \pm \mu_0 k_4 \cos^2 \theta_2 \end{aligned} \tag{2.3}$$

$$k_{12} = k_3 \sin\theta_1 \cos\theta_1 + k_4 \sin\theta_2 \cos\theta_2 \pm \mu_0 k_3 \cos^2\theta_1 \pm \mu_0 k_4 \cos^2\theta_2 \tag{2.4}$$

$$k_{22} = k_2 + k_3 \cos^2\theta_1 + k_4 \cos^2\theta_2 \tag{2.5}$$

$$F_1 = N_1 \sin\theta_1 - N_2 \sin\theta_2 \tag{2.6}$$

$$F_2 = N_1 \cos\theta_1 - N_2 \cos\theta_2 \tag{2.7}$$

in which $m$, $c_1$, $c_2$, $k_1$, $k_2$, $k_3$, $k_4$, $\theta_1$, $\theta_2$, $N_1$, and $N_2$ are defined in Figure 2.3. Also, $\mu_0$ is friction coefficient between brake shoe and drum. The ± sign in Equations (2.3) and (2.4) are related with sign function.

## 2.4. Therotical Modal Analysis

Equation of motion for undamped multi-degree of freedom system is written as

$$[M]\{\ddot{x}(t)\} + [K]\{x(t)\} = \{f(t)\} \tag{2.8}$$

where $[M]$ and $[K]$ are mass and stiffness matrices of the system, respectively. Also, $\{x(t)\}$ and $\{f(t)\}$ are displacement and force vectors of the system.

Equation (2.8) can be treated as a cantilever beam under force vector $\{f(t)\}$ as shown in Figure 2.4.

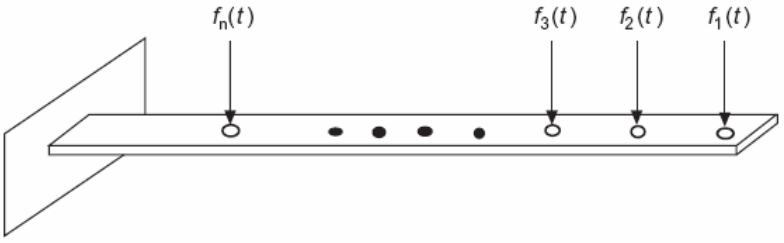


Figure 2.4. A cantilever beam under external force vector $\{f(t)\}$
(Source: He, 2001)

Therefore, considering the Figure 2.4, the following equations can be written

$$\{x(t)\} = \{x_1(t) \quad x_2(t) \quad \cdots \quad x_n(t)\}^T \tag{2.9}$$

$$\{f(t)\} = \{f_1(t) \quad f_2(t) \quad \cdots \quad f_n(t)\}^T \tag{2.10}$$

Displacements and force vectors can be written as function of sinusoidal function sin$\omega t$ due to the harmonic motion as follows

$$\{x(t)\} = \{X\} \sin \omega t \tag{2.11}$$

$$\{f(t)\} = \{F\} \sin \omega t \tag{2.12}$$

In Equations (2.9) and (2.10), $\{X\}$ and $\{F\}$ are time independed amplitudes of displacements and forces of the undamped multi-degree of freedom system.

By substituting Equations (2.9) and (2.10) into Equation (2.8), the following equation is obtained:

$$([K] - \omega^2[M])\{X\} = \{F\} \tag{2.13}$$

The first term with curved paranthesis at left hand side of Equation (2.13) is known as dynamic stiffness matrix and denoted by [$Z$(ω)], namely

$$[Z(\omega)] = [K] - \omega^2[M] \tag{2.14}$$

Thus, displacement amplitude vector $\{X\}$ is found by using the inverse of [$Z$(ω)] as

$$\{X\} = [Z(\omega)]^{-1}\{F\} \tag{2.15}$$

The inverse of [$Z$(ω)] is known as receptance FRF (Frequency Response Function) matrix of the multi-degree of freedom system and denoted by [$\alpha(\omega)$] which can be written in open form as

$$[\alpha(\omega)] = \begin{bmatrix} \alpha_{11}(\omega) & \alpha_{12}(\omega) & \cdots & \alpha_{1n}(\omega) \\ \alpha_{21}(\omega) & \alpha_{21}(\omega) & \cdots & \alpha_{21}(\omega) \\ \vdots & \vdots & \vdots & \vdots \\ \alpha_{n1}(\omega) & \alpha_{n1}(\omega) & \cdots & \alpha_{nn}(\omega) \end{bmatrix} \tag{2.16}$$

Depending on the subscript *ij* of $\alpha_{ij}(\omega)$, FRF is referred. If *i=j*, it is point FRF, otherwise it is transfer FRF.

It can obtained from Equation (2.15) and (2.16) that $X_i$ which is the displacement amplitude at coordinate *i* can be written as

$$X_i = \alpha_{i1}(\omega)F_1 + \alpha_{i2}(\omega)F_2 + \cdots + \alpha_{in}(\omega)F_n \tag{2.17}$$

It is seen from Equation (2.17) that $\alpha_{ij}(\omega)$ is related with the receptance FRF at point *i* due to the force acting on point *j*. As an illustration of point FRF, Figure 2.5 is given.

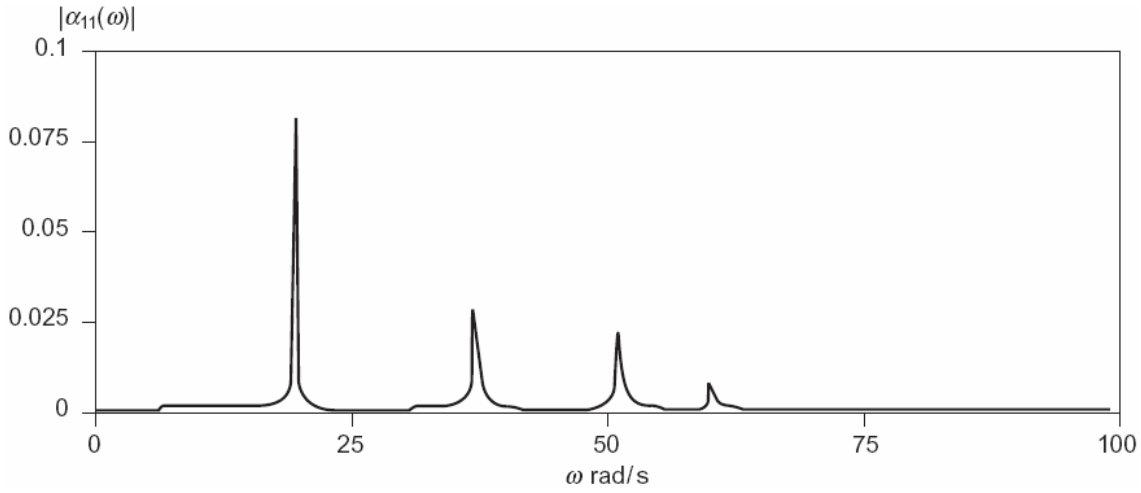


Figure 2.5. Receptance $\alpha_{11}(\omega)$ for the system shown in Figure 2.4.
(Source: He, 2001)

The mobility FRF $[Y(\omega)]$ and the accelerance FRF $[A(\omega)]$ are written as follows:

$$[Y(\omega)] = -j\omega[\alpha(\omega)] \tag{2.18}$$

$$[A(\omega)] = -\omega^2[\alpha(\omega)] \tag{2.19}$$

## 2.5. Experimental Modal Analysis

Experimental modal analysis of a structure requires several equipments. Arrangement of equipments for experimental modal analysis is illustrated in Figure 2.6.

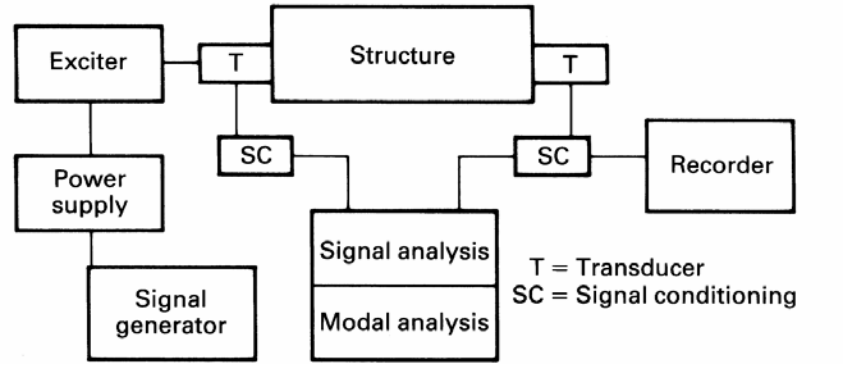


Figure 2.6. Arrangement of components for experimental modal analysis
(Source: Inman, 2006)

It is seen from Figure 2.6 that structure is in contact with transducers which transforms the motion to electrical signal. However, the outputs of transducers are needed amplification which is provided by signal conditioner. The signal analyzer receives the signal from signal conditioner and evaluates the signals by connecting the modal analyzer. Structure is excited to give a motion in two ways: either by using a shaker or by hitting a impact hammer. If a shaker is used, it is excited by signal generator via power supply. Signal generator provides different kind of excitation functions such as harmonic, ramped, impulsive etc. The excitation frequencies provided by an impact hammer is shown in Figure 2.7. It is seen from Figure 2.7 that the impact hammer having characteristics as in this figure is not effective the frequencies above $\omega_c$.

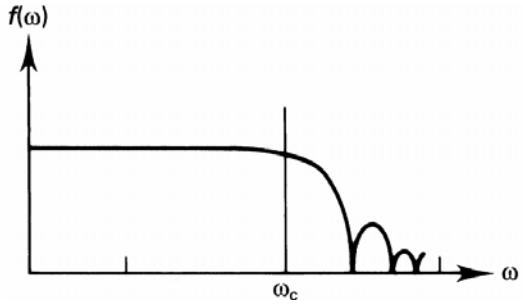


Figure 2.7. Frequencies excited by impact hammer
(Source: Inman, 2006)

The most critical equipments are transducers which are produced by using piezoelectric materials. If the transducer generates signals proportional acceleration, it is called as accelerometers.

Experimental modal analysis is done generally in frequency domain. In order to present this topic, it is necessary to start with expressing the periodic function $x(t)$ with period $T$ as Fourier series. It is given by Inman (2006) as follows:

$$x(t) = \frac{a_0}{2} + \sum_{i=1}^{\infty}\left[ a_i \cos\frac{2\pi i t}{T} + b_i \sin\frac{2\pi i t}{T} \right] \tag{2.20}$$

where $a_i$ and $b_i$ are known as Fourier coefficients and given by the following equations

$$a_i = \frac{2}{T}\int_0^T x(t)\cos\frac{2\pi i t}{T}dt \tag{2.21}$$

$$b_i = \frac{2}{T}\int_0^T x(t)\sin\frac{2\pi i t}{T}dt \tag{2.22}$$

Some periodic functions and their Fourier spectrums are given in Figure 2.8.

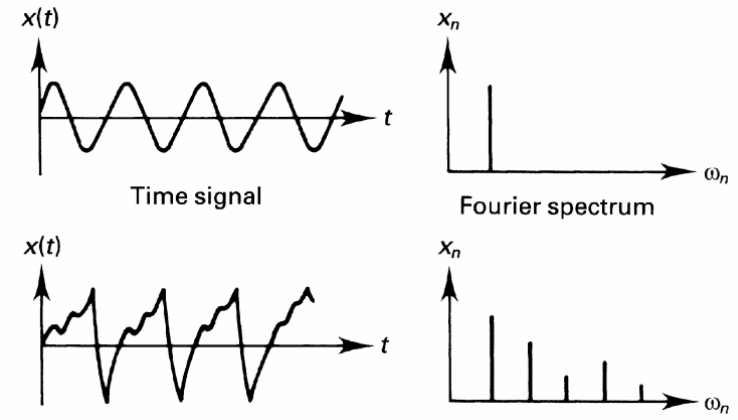


Figure 2.8. Frequency signal and FFT spectrum plots
(Source: Inman, 2006)

In practice, continuous function is recorded in discrete form. In this case, continuous function $x$(t) is represented by discrete form as $\{x(t_k)\}$, $k$=1,2,…$N$, where $N$ is the number of data to represent the continuous function $x$(t). Figure 2.9 illustrates this process.

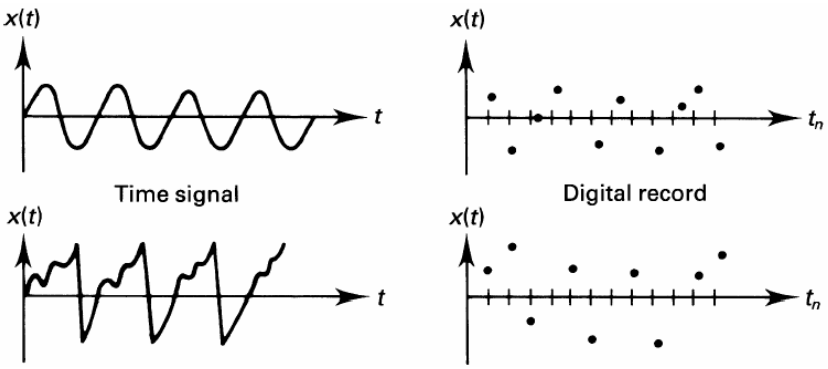


Figure 2.9. Continuous functions $x(t)$ and their discrete forms
(Source: Inman, 2006)

After having discrete form of the function $x(t)$, the discrete Fourier transform can be obtained.

$$x_k = x(t_k) = \frac{a_0}{2} + \sum_{i=1}^{N/2}\left[ a_i \cos\frac{2\pi i t_k}{T} + b_i \sin\frac{2\pi i t_k}{T} \right], \quad k = 1,2,....,N \tag{2.23}$$

where $a_i$ and $b_i$ given as

$$a_0 = \frac{1}{N}\sum_{k=1}^{N} x_k \tag{2.24}$$

$$a_i = \frac{1}{N}\sum_{k=1}^{N} x_k \cos\frac{2\pi i k}{N} \tag{2.25}$$

$$b_i = \frac{1}{N}\sum_{k=1}^{N} x_k \sin\frac{2\pi i k}{N} \tag{2.26}$$

Equation (2.23) is written in matrix form in term of the unknown coefficients vector $\{a\}=\{a_1, a_2, \ a_{N/2}, b_1, b_2, \ldots b_{N/2}\}^{\mathrm{T}}$ as

$$\{x\} = [C]\{a\} \tag{2.27}$$

Therefore, unknown coefficients vector $\{a\}$ is found as

$$\{a\} = [C]^{-1}\{x\} \tag{2.28}$$

The computing $[C]^{-1}$ is called FFT (Fast Fourier Transform).

## 2.6. Finite Element Model

Finite element method is a very common numerical method in solid mechanic problems. This method has been developed since 1960 (Cook 1989). It is based on Rayleigh-Ritz method (Reddy 1993). However, Rayleigh-Ritz method is applied for each finite element. The idea of finite element is related with the dividing the geometrically complex shape to simple ones such as bar, beam, curved beam, plate, etc since the problem associated with simple geometrical shape is solvable analitically or numerically in simple approaches such as Rayleigh-Ritz method.

Finite elements used to model a geometrical shape are connected to each other with its extremities called as nodes. For examples: bar element has nodes at its ends, triangular element has nodes at its corners. However, to increase the accuracy of finite elements, internal nodes can be added. Physical parameters related with the problem are state variables at nodes. Thus, displacements are the nodal variables in solid mechanics applications. Division of the whole geometrical shape is called as meshing. Meshing of the geometrical shape is extremly important step for finite element analysis. It requires convergency studies by selecting different element sizes and solving the problem for each selected element sizes.

Each finite element has characteristics stiffness, mass, and damping matrices in vibrations. Combination of element matrices are based on the continuity conditions of the state variables at nodes and is known as assembling. After assembling of the finite element matrices, the global characteristics are obtained. Boundary conditions are applied to global characteristics matrices. (Yardimoglu, 2015)

The matrix form of the free vibration equation for multiple degrees of freedom system is given as follows:

$$[M]\{\ddot{x}(t)\} + [C]\{\dot{x}(t)\} + [K]\{x(t)\} = \{f(t)\} \tag{2.29}$$

where [$M$], [$C$], and [$K$] are mass, damping, and stiffness matrices, respectively. In Equation (2.29), $\{x(t)\}$ and $\{x(t)\}$ are displacement and force vectors, respectively.

In order to simplify the vibration analysis, the damping matrix [$C$] is considered as linear combination of stiffness matrix [$K$] and mass matrix [$M$]. This type of damping is known as Rayleigh or proportional damping (Yardimoglu, 2015) and expresses as

$$[C] = \alpha\ [M] + \beta [K] \tag{2.30}$$

where $\alpha$ and $\beta$ are proportionality constants.

Modal analysis of multiple degrees of freedom system is done by using the following equation

$$([K] - \omega_i^2 [M])\{u_i\} = \{0\} \tag{2.31}$$

where $\omega_i$ is $i^{th}$ eigenvalues which corresponds to $i^{th}$ natural frequency and $\{u_i\}$ is the $i^{th}$ eigenvector which corresponds to mode shape vector.

ANSYS solves Equation (2.31) by using the methods listed below:

- Block Lanczos (default) method is employed for large symmetric problems.
- Subspace method is utilized for large symmetric problems too.
- Power Dynamics method is made use of very large models.
- Reduced (Householder) method is based on reduced system matrices.
- Unsymmetric method is proper to unsymmetric matrices.

In this study, default one is selected.

# CHAPTER 3

# FINITE ELEMENT ANALYSIS

## 3.1. Finite Element Analysis of Drum Brakes

In Chapter 2, theory of modal analysis is given. Such a noise and vibration investigation, numerical solution is obtained by finite element method based on modal analysis. In this subsection, finite element model of drum brake is discussed. Friction induced noise pairs can be described as shoes assemble and drum shown in Figure 3.1. Shoe has three main parts which are lining materials, rims, and webs. First of all, each part is modelled in ANSYS for modal analysis. There are no geometrical simplification on drum, lining material and shoes such as removing the fillets etc. CAD models are generated in nominal dimensions. Geometric dimensions of drum are given in Table 2.1. Then, finite element model of drum is obtained.

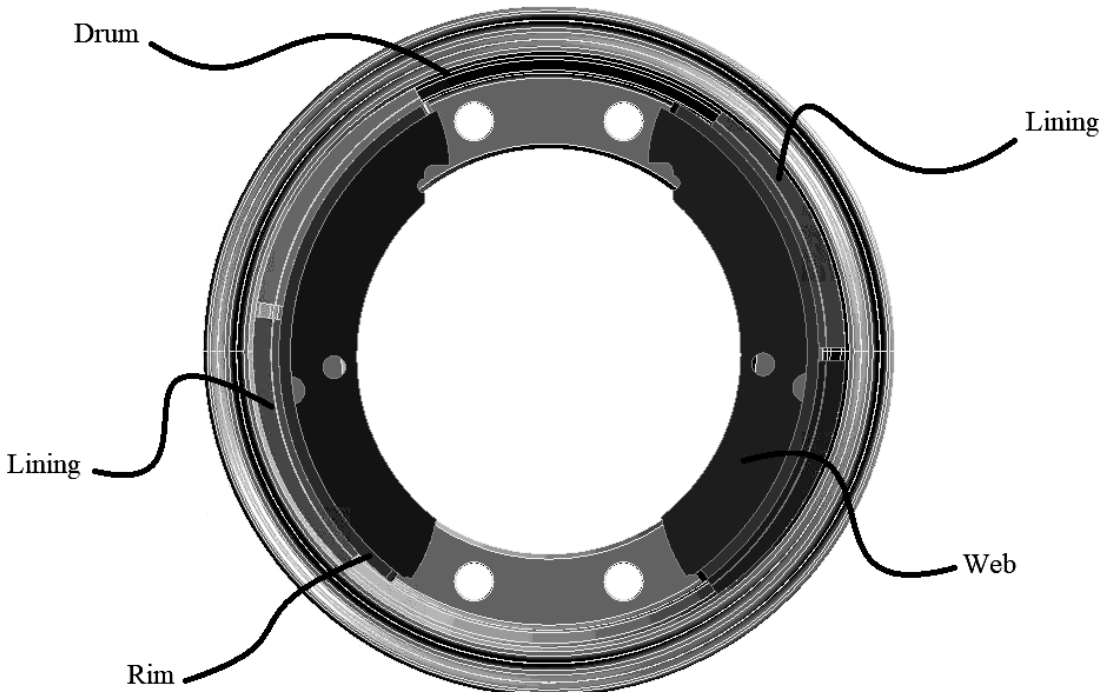


Figure 3.1. Definition of friction pairs

The important dimensions of drum are inside diameter, outside diameter, offset of drum brake, thickness of flange surface, outside diameters given in table 3.1. Additionally, mass of drum is 67.883 kg.

Table 3.1 Geometrical definition of drum

| Geometric entity | Dimension |
|---|---|
| Inside diameter | 410 mm |
| Offset | 275 mm |
| Outside diameter 1 | 453 mm |
| Outside diameter 2 | 457 mm |
| Outside diameter 3 | 479 mm |

For finite element model, drum material is selected as gray cast iron. Mechanical properties of gray cast iron are given in Table 3.2.

Table 3.2 Mechanical properties of gray cast iron

| Mechanical properties | Dimension |
|---|---|
| Density | 7200 kg.m3 |
| Young's modulus | 170 GPa |
| Poisson's ratio | 0.29 |
| Yield tensile strenght | 172 MPa |
| Ultimate tensile strength | 700 MPa |

Stress and strain curve is modelled as multilinear plot as seen in Figure 3.2. Tensile test specimen is taken out from drum.

ANSYS Workbench is used for modal analysis. Element and nodes are studied as a case study for optimum mesh quality and minimum errors. Table 3.3 shows the case studies for mesh of drum. The format of the case study notation as follows: CS are the initials of "Case Study", first number like 1, 2, and 3 indicates the case study number, and last number refers to element size.

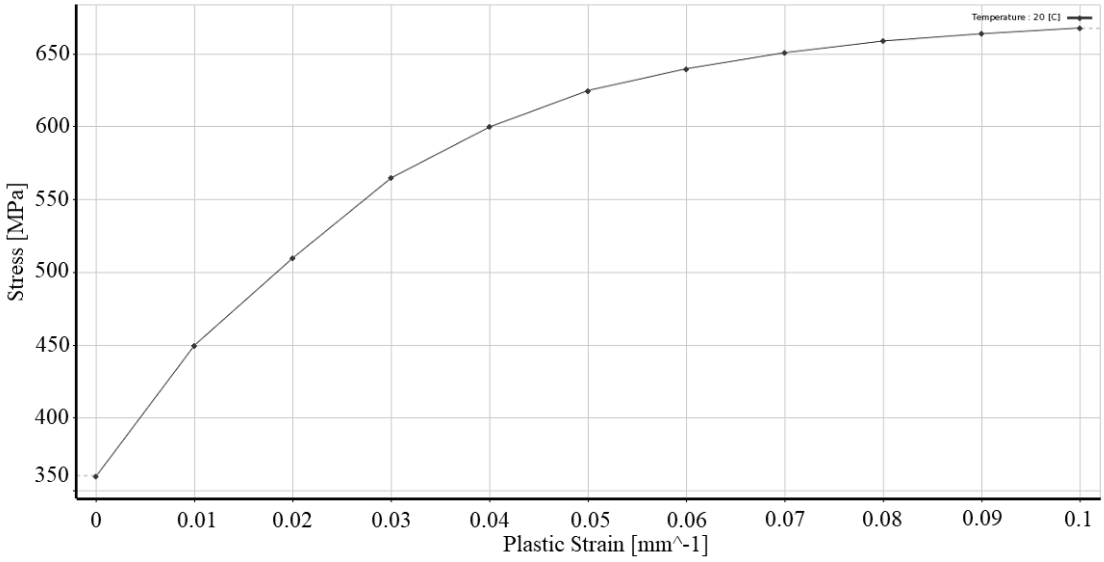


Figure 3.2. Stress and Strain curve of gray cast iron for FEA

Table 3.3 Case study of mesh for drum

| Case study | Element | Number of element | Number of node |
|---|---|---|---|
| CS18 | SOLID186 | 11026 | 202865 |
| | SOLID187 | 48151 | |
| CS26 | SOLID186 | 90012 | 372533 |
| | SOLID187 | 15441 | |
| CS34 | SOLID186 | 229326 | 944926 |
| | SOLID187 | 24869 | |

In finite element analysis, three types of case are studied as CS18, CS26, and CS34. In order to obtain as possible as accurate results, solid elements are used. The selected solid elements for CS18 are SOLID186 having 20 nodes and 3 degree of freedoms and SOLID187 having 10 nodes and 3 degree of freedoms. Selecting the finite element size as 8 mm due to the CS18, drum is meshed by 11026 SOLID186 and 48151 SOLID187, namely totally 59177 elements are used. In this case, the corresponding number of node is 202865. In the second case study, CS26, element size is set to 6 mm. Thus, the model has 90012 and 15441 elements for SOLID186 and SOLID187, respectively. In this case total number of element and node are 105453 and 372533, respectively. Similar to CS18 and CS26, details of CS34 can be read from Table 3.3. Element types are given in Figure 3.3.

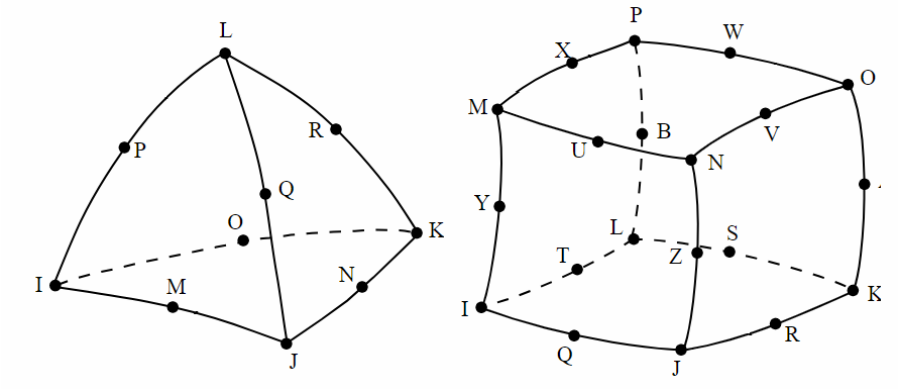


Figure 3.3. Types of mesh
(Source: Sharcnet, 2018)

The CPU times and differences with respect to experimental results, given in next Chapter, are given in Table 3.4 for three case studies. It is clear from table 3.4 that CS1 has minimum CPU which is critical for industrial applications.

Table 3.4 CPU time and errors for drum

| Case study | CPU | Difference |
|---|---|---|
| CS18 | 296 | %3-4 |
| CS26 | 661 | %1.5-2 |
| CS34 | 8968 | %1.5-2 |

Meshing procedure in ANSYS Workbench is given as follows: Meshing setup of drum is set for solid element. Size function is kept as default setting. Relevance center is setup as coarse mesh. Revelence center controls the size of element by changing number between -100 and +100. In this scale, course is reflected by -100. It can be possible to prevent high number of elements by adjusting the revelence center. Transition between elements has fast option. Span angle control the elements which divide a radius feature. Center of span angle is arranged as medium. The minimum edge length result is 0.528 mm with this meshing setup. The result of meshing can be shown in Figure 3.4 for drum.

The resultant natural frequencies of drum are given in Table 3.5. The noise is occured at low frequencies. Because of that reason, the first 5 natural frequencies are given in Table 3.5. Modes shapes are given in Figure 3.5.

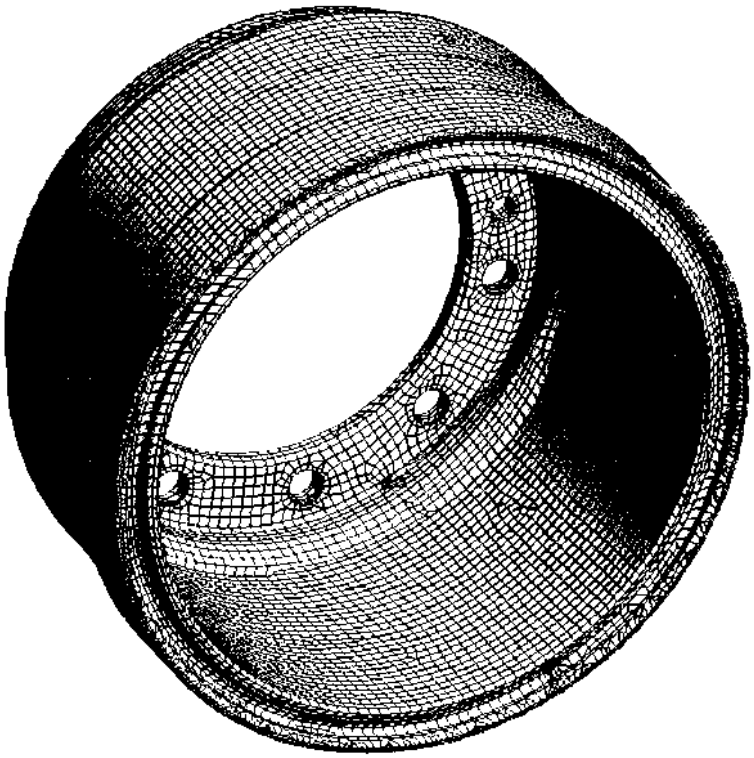

Figure 3.4. Finite element model of drum

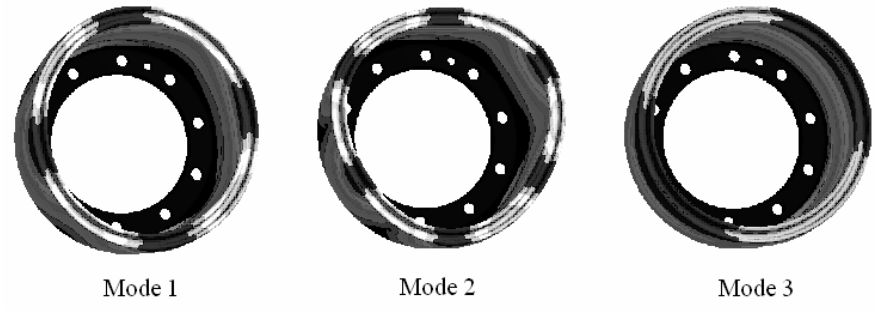


Figure 3.5. Mode shapes for drums

The critical geometrical definition of lining is outside diameter. Because it is assummed that lining material has bedding to use in its place. The outside diameter of assemble is 410 mm. The properties of lining material are not given here due to the commercial reasons. Change of stiffness and mass are neglected because of that the natural frequencies of shoes are so close for each lining material. Mechanical properties of rim and web, made of ST37, are given in Table 3.6. Method of obtaining stress and strain curve is as the same with drum. It can be shown in Figure 3.6.

Table 3.5 Modal analysis results for drum

| Mode numbers | Frequencies [Hz] |
|---|---|
| 1 | 704.01 |
| 2 | 1197.1 |
| 3 | 1266.2 |

Table 3.6 Mechanical properties of ST37

| Mechanical properties of material | Value |
|---|---|
| Young's modulus | 200 GPa |
| Poisson's ratio | 0.3 |
| Yield tensile strenght | 350 MPa |
| Ultimate tensile strength | 420 |

For lining material and shoe assemble, the case studies studies for determination of the mesh quality and CPU time are given in Table 3.7. The solid elements of shoe assemble are same as drum. Stress and Strain curve of ST37 for FEA is used for Ansys bilinear material model. However, two types of contact elements CONTA174 and TARGE170 shown in Figure 3.7 are used for lining and drum interactions.

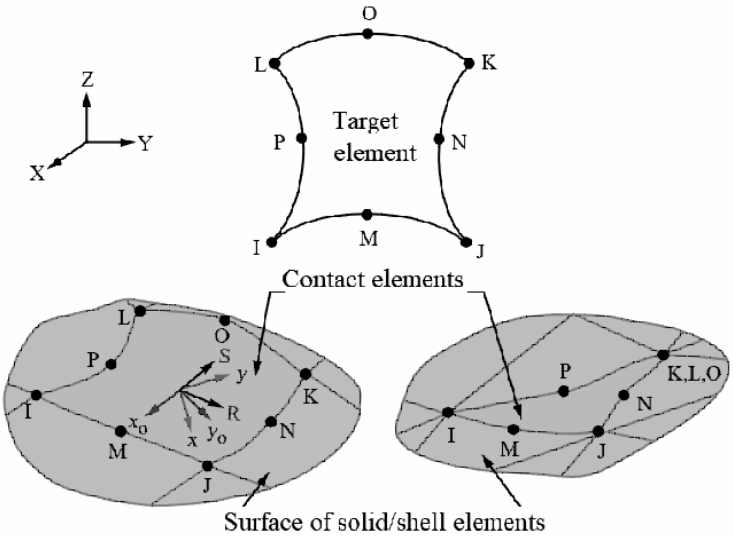


Figure 3.6. Element types for contact surface
(Source: Sharcnet, 2018)

Table 3.7 Case study of mesh for shoe

| Case study | Element | Number of element | Number of node |
|---|---|---|---|
| CS18 | SOLID186 | 17163 | 76462 |
| | SOLID187 | 5756 | |
| | TARGE170 | 3947 | |
| | CONTA174 | 3947 | |
| CS26 | SOLID186 | 27980 | 120606 |
| | SOLID187 | 5990 | |
| | TARGE170 | 6077 | |
| | CONTA174 | 6077 | |
| CS34 | SOLID186 | 9724 | 267717 |
| | SOLID187 | 61733 | |
| | TARGE170 | 11888 | |
| | CONTA174 | 11888 | |

Setup of mesh is similar with drum. The finite element model is given in Figure 3.8.

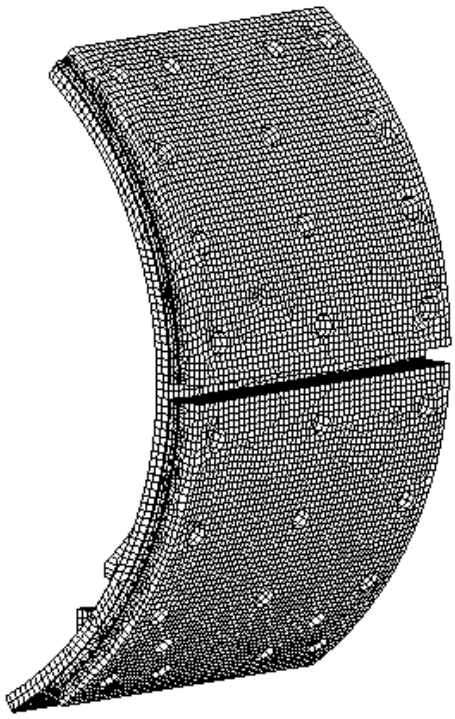

Figure 3.7. Finite element model of shoe

Contact pairs which are rim and web are connected with bonded contact method. This method is useful for welded parts. The other pairs are lining material and rim. The frictional contact is selected. Friction coefficient is 0.37. In addition to these, rivets are modelled. Whole rivets are bonded to rim and they have frictional contact with lining material. Friction coefficient is the same. Mesh CPU times and differences with respect to experimental results are given in Table 3.8. The case study 3, CS34, is choosen for modal analysis of shoe.

Table 3.8 CPU time and errors for shoe

| Case Study | CPU | Difference |
|---|---|---|
| CS18 | 42 | >5% |
| CS26 | 83 | 3-4% |
| CS34 | 274 | <2.5% |

The natural frequencies of shoes are given in Table 3.9. Also, mode shapes of shoes are illustrated in Figure 3.9.

Table 3.9 Modal analysis results for shoe

| Mode numbers | Frequencies [Hz] |
|---|---|
| 1 | 614.5 |
| 2 | 1158.6 |
| 3 | 1436.8 |

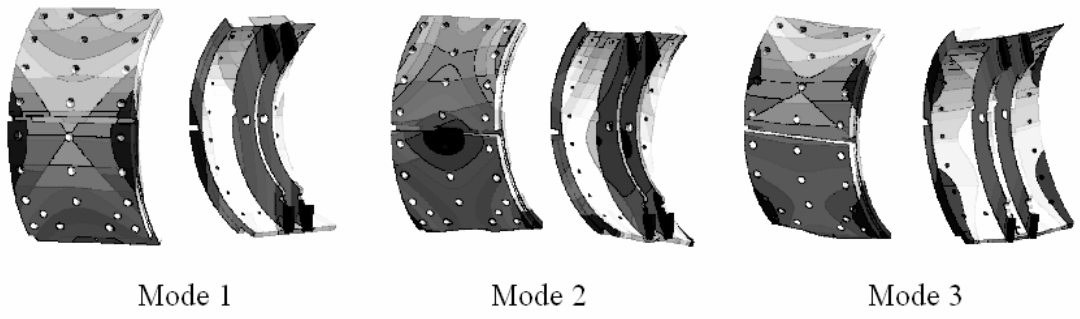


Figure 3.8. Mode shapes for shoes

Additionally, assemble of drum and shoe is studied in finite element analysis. Its finite element model is shown in Figure 3.10. Abutment and piston surfaces of shoes have constraints that both of them can not move in horizontal directions. Also, inner diameter surface of drum has only rotational freedom about its axis.

Coulomb's friction law with constant coefficient is used. The friction coefficient between shoe and drum is measured 0.37 at generally under 30°C.

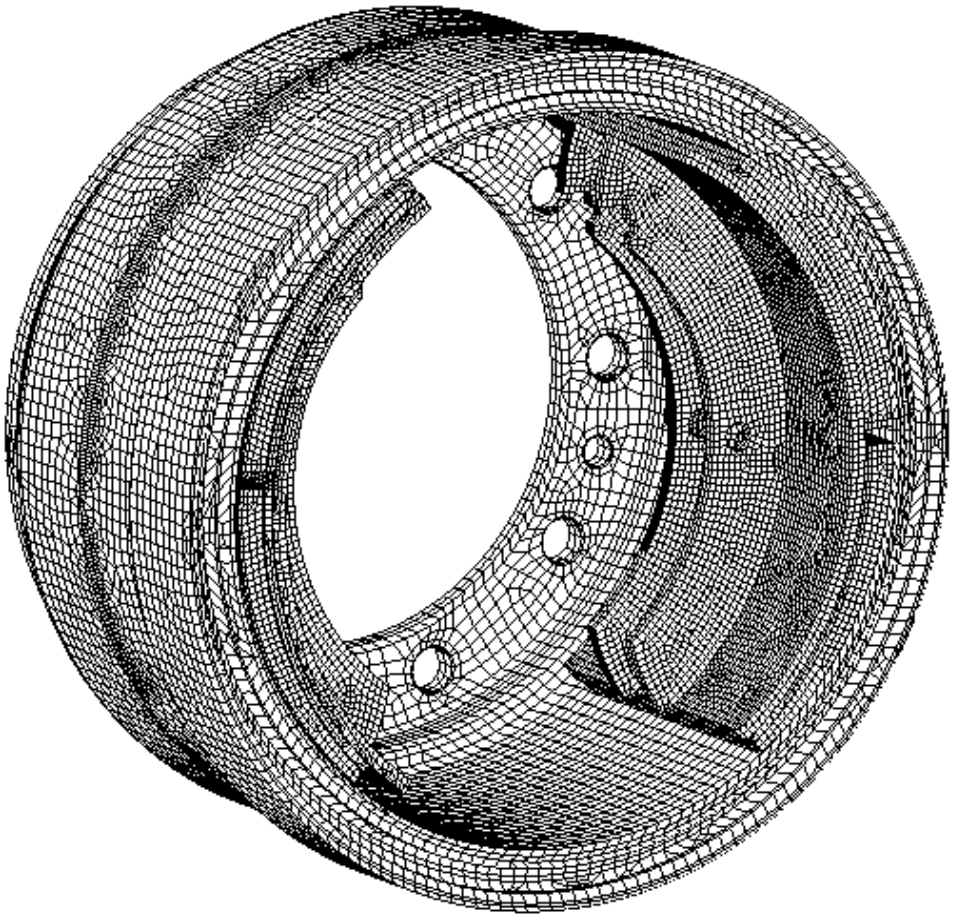

Figure 3.9. Finite element model of shoe and drum interaction

Lining material is also modelled as they are fully contact with drum. The roughness of drum is neglected. There is no balance in the drum. All dimensions are nominal.

The natural frequencies of the system given in Figure 3.10 are given in Table 3.10.

Table 3.10 Modal analysis results for brake

| Mode numbers | Frequencies [Hz] |
|---|---|
| 1 | 722.9 |
| 2 | 1254.8 |
| 3 | 1297.1 |
| 4 | 1332.8 |

Mode shapes of the system are given in Figure 3.11.

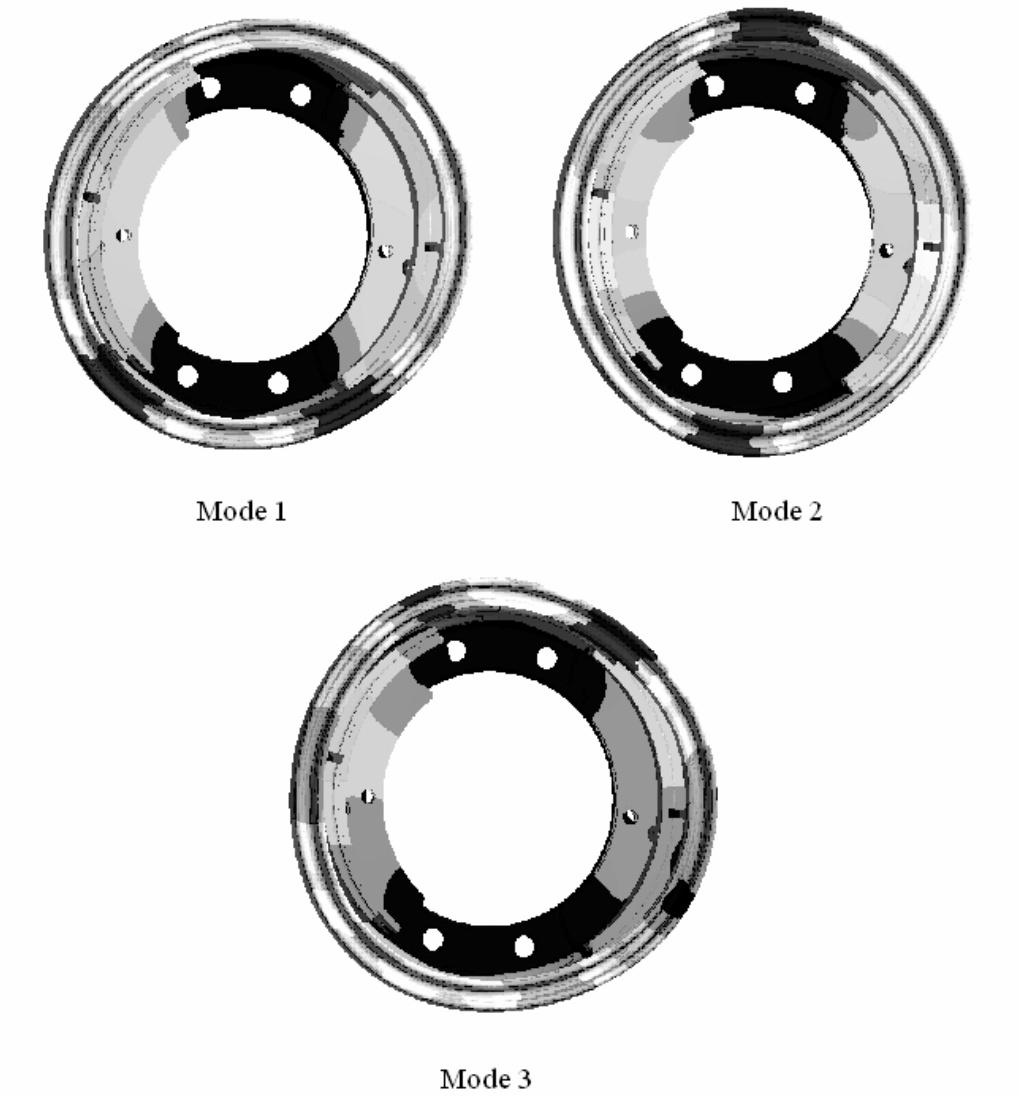


Figure 3.10. Mode shapes for shoe and drum interaction at 0 Bar

# CHAPTER 4

# EXPERIMENTAL ANALYSIS

## 4.1. Experimental Setup for Brake Dynamometer

Theories are given in Chapter 2 for modal analysis and testing. Frequency responce function or transfer function methodology is used in this section for dynamometer tests. The same testing procedure is used for different temperature conditions. Coulomb's friction law is used for constant friction coefficient for each test. However, it is change with respect to temperature. There are four main subsystems which are dynamometer, measurement system, brake parts and vehicle's parts which are needed to supply connection of brake and create friction pairs. Brake parts and drum are discussed in Chapter 2 and 3. All instruments are calibrated and the errors of measurements are known. For the brake components, all measurements are obtained in tolerance limit. Unbalanced drum is used. The inner surface of drum has a roughness value which is in tolerance limit. All tests are occurred at room temperature at 32-34°C. Humidity is %37-40. Little change of temperature and humidity is neglected.

### 4.1.1 Brake Dynamometer

Brake dynamometer is designed for disc brakes and drum brakes of heavy commercial vehicle. There are several types which are industrial usage such as performance dynamometer, NVH dynamometer and etc. In this thesis, a performance dynamometer is used. Technical information for dynamometer can be described that it has 1392 $kg.m^2$ moment of inertia. This moment of inertia simulates fully laden heavy commercial vehicle. For cooling, a fan transfers air from environment to brake drum. In addition to these, output of measurement can be described as velocity, temperature, and torque. Torque is measured by a fixture which is a torque arm and loadcell. Rotational velocity is converted to vehicle velocity. Brake is mounted to dynamometer by cylindrical fixture instead of axon and hub. Dynamometer is shown in Figure 4.1.

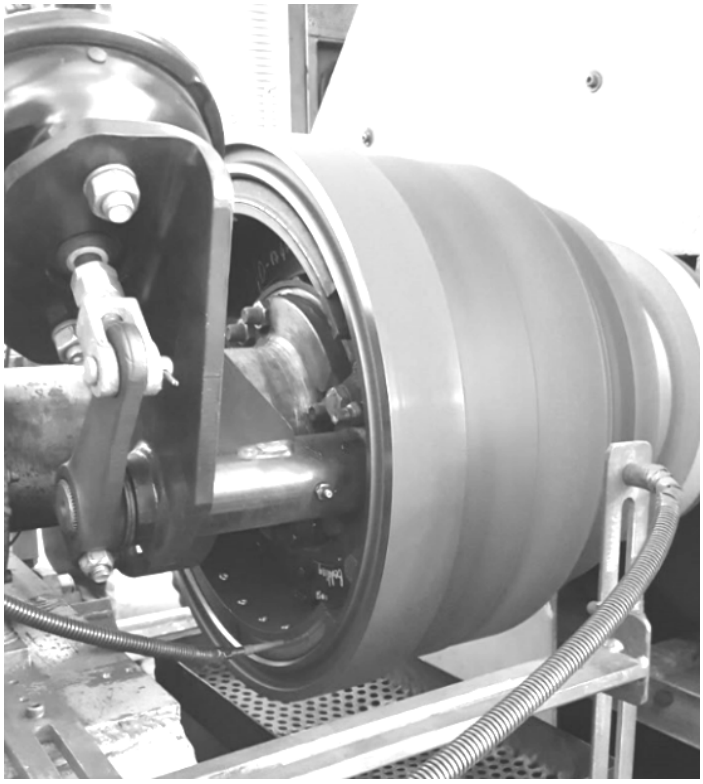

Figure 4.1. Dynamometer of drum brake

### 4.1.2 Impact Hammer

In modal analysis, Dytran 5800B4 impulse hammer shown in Figure 4.2 is used. There are different types of instrument to give first impulse. Medium stiffness of impact tips is selected for this investigation.


Figure 4.2. Impact hammer
(Source: Dytran, 2018)

### 4.1.3 Pressure Sensor

UNIK 5000 Series automotive pressure transducers shown in Figure 4.3 are used to obtain input pressure of air chamber. Pressure sensor's variant is amplified. It has 25 mm diameter and it is stainless steel. Output signal is converted from 0 to 10V. Connector of pressure is male and it has G1/2 finish cut. In order to obtain accurated results, accuracy is ±0.04%. It's resistance to temperature is between -40°C and 80°C.

Figure 4.3. Pressure sensor
(Source: Gemeasurements, 2014)

### 4.1.4. Microphone

In the noise measurements, ½ inc ICP Microphone Preamplifier is preferred. The range of measurements is up to 120 dB. If the frequency is between 10 Hz and 20 kHz, response of frequency can be changeable ± 0.1 dB. Operation temperature is identified between -10°C and +50°C. In order to obtain accurate results, humidity should be between 0 and 90% RH. The microphones are shown in Figure 4.4.

Figure 4.4. Microphone
(Source: Norsonic, 2007)

### 4.1.5 Temperature Sensor

K type thermocouples are used to measure lining material temperature. Connection of thermocouple is male connection which is standard. It can measure the temperature from 0°C to 1260°C. For high humidity which means that has continueing oxidizing, it could be used until 538°C temperature. Deviation of measured data is ±2.2.

### 4.1.6 Vibration Sensor

Model 7120A accelerometer shown in Figure 4.5 has wide bandwith to 10 kHz 10-32 side connector miniature cube. It is availible the dynamic range between ±50g and ±500g. It can measure frequency until 37 kHz. The phase response is in range between 1-3000 Hz. It resists the high and low temperature has range +100°C and -55°C. It was used for modal testing, vibration analysis and laboratory testing.


Figure 4.5. Vibration sensor
(Source: Disensors, 2010)

### 4.1.7 Data logger

Measurements are saved by data logger named IMC CRONOS. It has a connection of Ethernet with computer. Data can be collected as analog and digital. There are six modules in the whole system. One of them is CRONOSflex which is power supply for main module of the data logger. Connector of module has 20 pins. It is necessary for test of vehicle. The other module of data logger is CRFX/ISO2-16-2T shown in Figure 4.6. This equipment is for K type of thermocouple. There are 16 female channels. Rate of sampling is maximum 10 kHz. In experimental theory in Chapter 2, antianalyzing is discussed. For

these module, filter which is digital has frequency level between 10 Hz and 500 Hz. Range of measurements are between -200°C and +1200°C. Additionally, CRFX/AUDIO2-4 is used for noise and vibration measurements. It is the same same rate of sampling with temperature module. Range for measurement is up to 49 kHz. By using low pass filter, this frequency range can be setted between 50 Hz and 20 kHz. Resolution is same with the other modules. It can be measured noise up to 106 dB. DSUB-15 connectors are used for connection of insturements to data logger.

### 4.1.8 Signal Analyzer

In signal analysis, IMC Famos is used. It means that fast analysis and monitoring of signals.In famos digital input is converted from time domain to frequency domain by using Frequency Response Function. Frequency domain and acceleration graphs are examined. The noisy parts of these results are cutted out by using Famos. They are also examined by spectrum analysis. In addition to these, generally frequency domain and amplitude graphs are used.

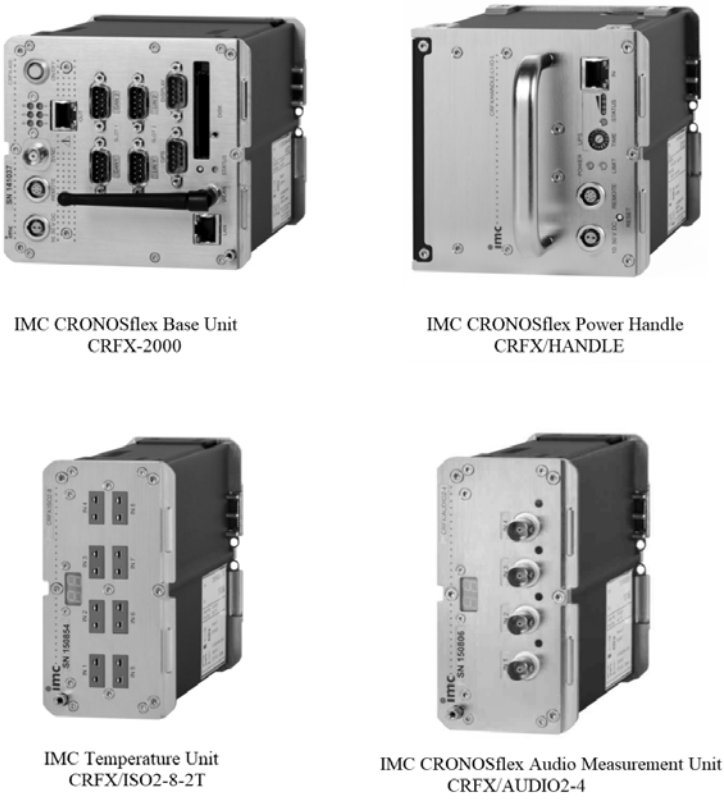


Figure 4.6 Data logger (Modified)
(Source: IMC, 2013)

## 4.2. Procedure and Results of Modal Testing

In modal testing of drum and shoe, boundry conditions are considered. Drum is assembled to hub and there are no forces on it. Shoe is also assembled to brake. For accurate results, all tests are repeated for 10 times. The results are average values of these measurements. The modal testing results of drum and shoes are given in Table 3.10 and Table 3.11, respectively.

Table 4.1 Modal testing results for drum

| Mode numbers | Frequencies [Hz] |
|---|---|
| 1 | 727.7 |
| 2 | 1164.7 |
| 3 | 1214.8 |

Table 4.2 Modal testing results for shoe

| Mode numbers | Frequencies [Hz] |
|---|---|
| 1 | 633.8 |
| 2 | 1171.6 |
| 3 | 1494.1 |

## 4.3. Test Procedure and Results for Brake Dynamometer

In dynamometer, a vibration sensor which is numbered as 2 in Figure 4.7 is located on brake spider. Pressure sensor which is shown as 3 is fitted air chamber by using coupling. Thermocouple which is demonstrated as 1 in the Figure 4.7 is placed into lining material. Two microphones which are presented as 4 in the Figure 4.7 are used in dynamometer tests. One of them is standed inside cabin; the other was outside of the cabin. Enviroment noise is separated from noise which is measured inside dynamometer.

Brake dynamometer setup is given in Figure 4.7. In addition to this, assemble of brake and sub-assemble of dynamometer is shown.

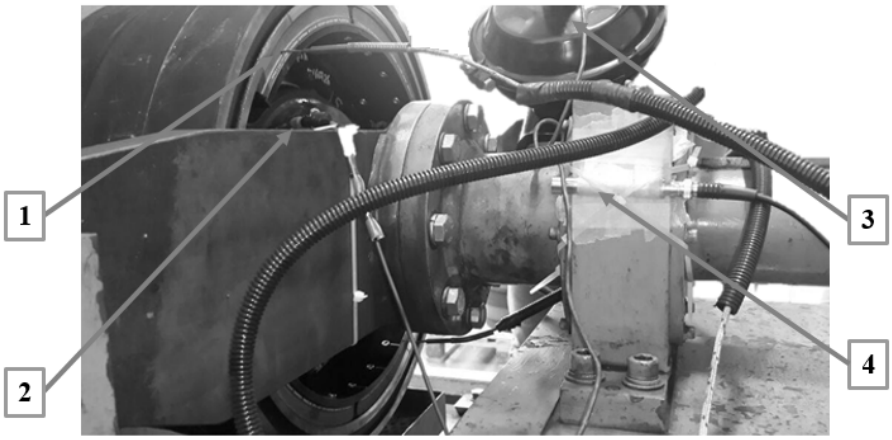


Figure 4.7. Setup of brake dynamometer

The last microphone is putted on cover of dynamometer shown in Figure 4.7.


Figure 4.8. Installation of 2nd microphone

When instrumentation of brake dynamometer is completed, all insturements are connected data logger and computer. Some values are also examined from dynamometer. They are temperature, velocity and torque.

After that, a test procedure is prepared. There are changing parameters in the design of experiment. They are velocity, pressure, temperature and material of linings. Lining material change also effects friction coefficient between shoe and drum interaction. Four different BS (Braking Situations) are considered for tests. They are written as BS on next pages. Each BS has three parts. Each part has ten tests because of repeatablitiy. In addition, accuracy also can be examined from these repetitive tests.

For each BS, velocity is shown in Figure 4.9. There are three types of velocity change with respect pressure. Three types of velocity is selected. But noisy part is at 20 m/s.

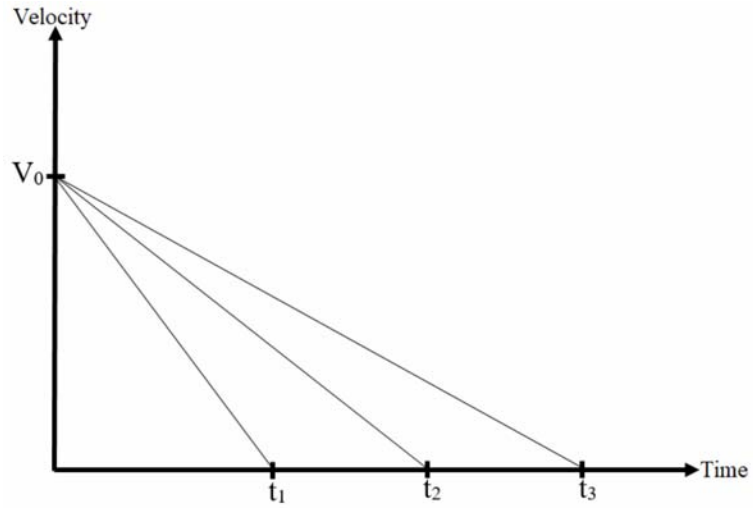


Figure 4.9. Velocity change for BS

Additionally, second parameter which is examined in the experiments of brake squeal is pressure. It is presented as $P_{max}$ in the Figure 4.10. Values are given in Table 4.3.

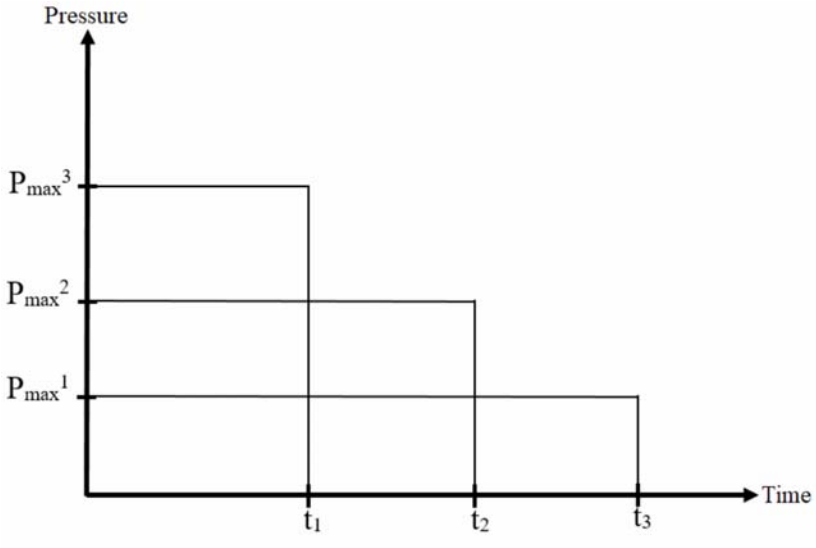


Figure 4.10. Pressure change for each BS

Temperature is constituted as a constant for each braking situtation. But, it should be considered that temperature is also changeable parameter. The last one is material change of linings. But its' technical detail is not given in this thesis. There are two types of composite lining material. One of them has more metallic composition. The other material

has no metal in the composition. So, friction coefficient change is focused on in the material of lining. Characteristic of friction coefficient for material 1 is given in Figure 4.11.

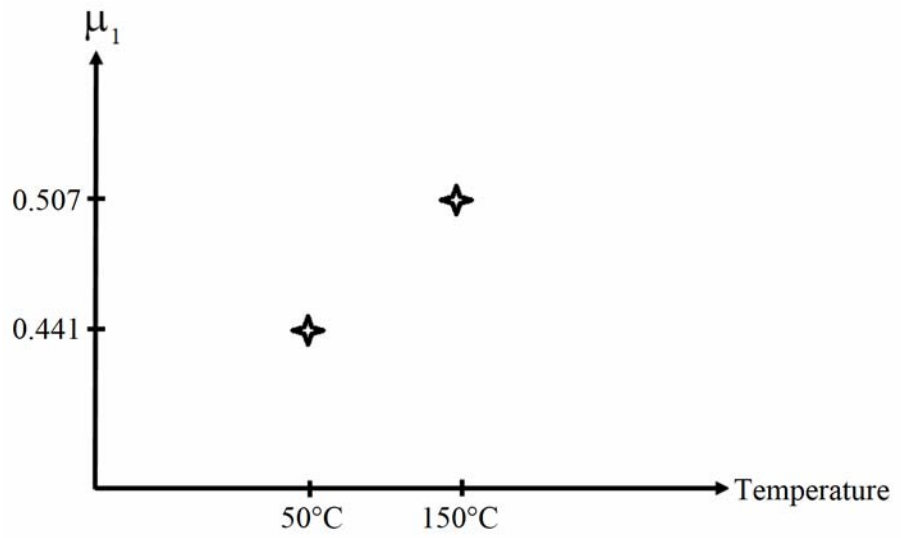


Figure 4.11. Friction coefficient change for material 1

Coefficient of friction for material 2 with respect to temperature is given in Figure 4.12.

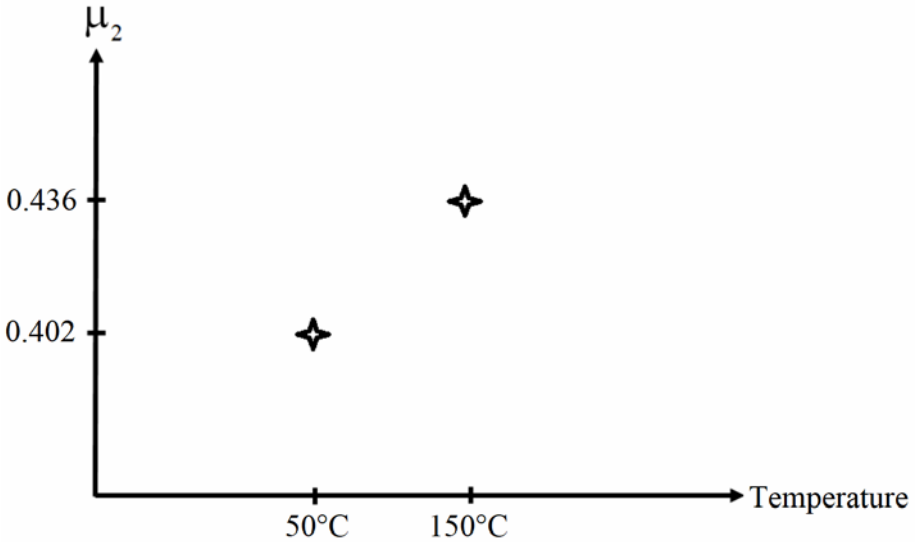


Figure 4.12. Friction coefficient change for material 2

All values of braking situations are given in below. In this experiment final velocities and are not considered. Noisy parts of whole experiment are focused on. Velocity is given above.

Table 4.3 Braking situations and parameters

| Braking Situation | $P_{max}$ | $T$ | Lining material |
|---|---|---|---|
| BS1 | 2 | 50 | M1 |
| | 4 | 50 | M1 |
| | 6 | 50 | M1 |
| BS2 | 2 | 150 | M1 |
| | 4 | 150 | M1 |
| | 6 | 150 | M1 |
| BS3 | 2 | 50 | M2 |
| | 4 | 50 | M2 |
| | 6 | 50 | M2 |
| BS4 | 2 | 150 | M2 |
| | 4 | 150 | M2 |
| | 6 | 150 | M2 |

First of all, BS1 and BS2 are considered in the experiments. The vibration results are given in Figure 4.13. The vibration and noise amplitude under 30 dB are not considered.

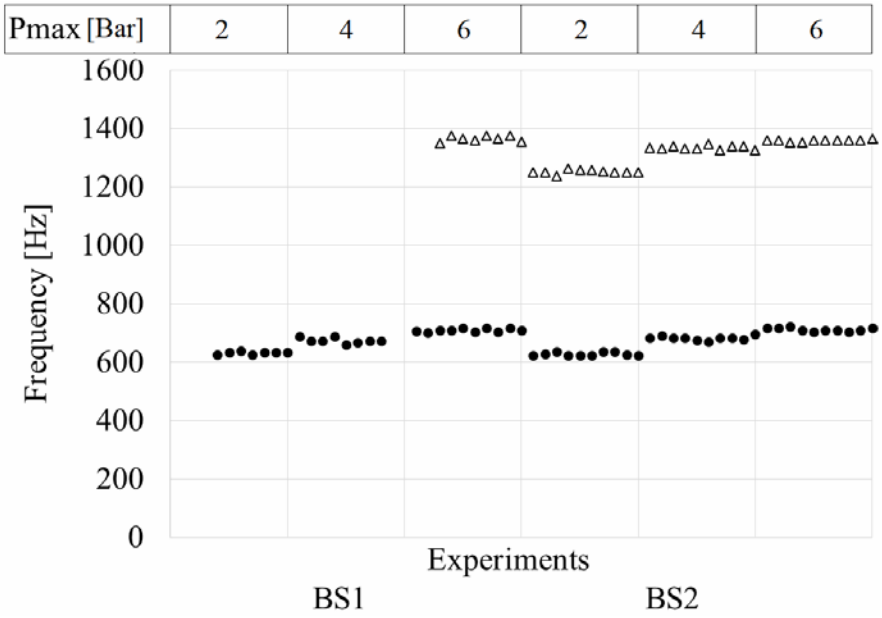


Figure 4.13. Vibration measurements for BS1 and BS2

Secondly, BS3 and BS4 are studied. The results are given in Figure 4.14. The vibration and noise amplitude under 30 dB are not considered as before.

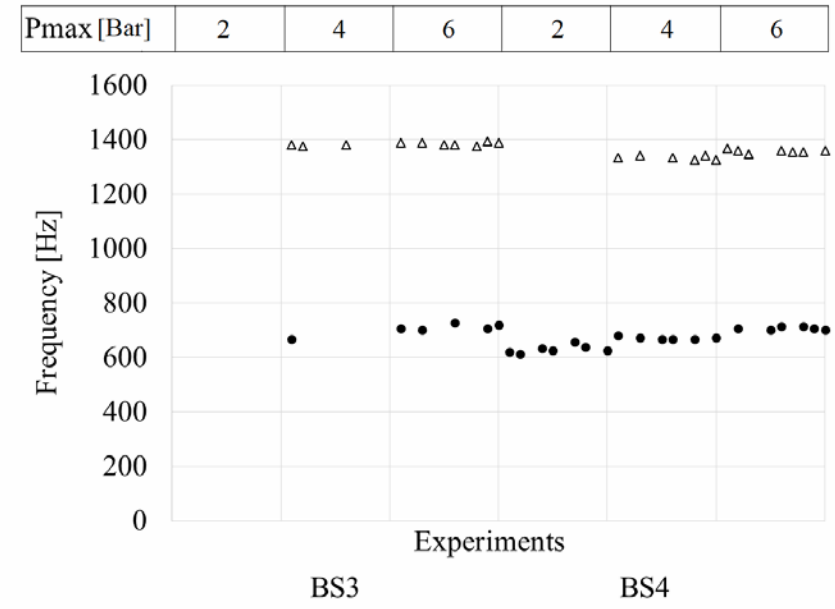


Figure 4.14. Vibration measurements for BS3 and BS4

One of the signal analysis results related with experiment of BS3 for $P_{max}$=4 bar is given in Figure 4.15. It is seen from this figure that damped frequencies are close to 649.8 Hz and 1362.6 Hz.

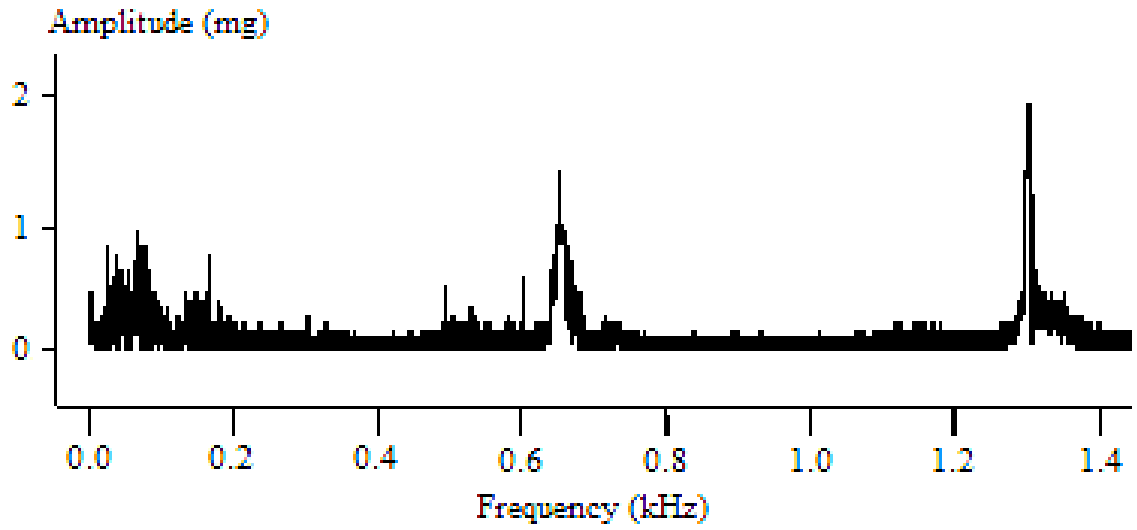


Figure 4.15. Frequency and amplitude graphs

## 4.4. Sound Measurements

The four vibration modes of brake system are given in Table 3.10. The maximum noise value is measured as 76 dB in BS2 for $P_{max}$=6 bar which corresponds to 1346.3 Hz. Another critical maximum noise value is measured as 46 dB in BS4 for $P_{max}$=6 bar which corresponds to 1362.3 Hz.

# CHAPTER 5

# CONCLUSION

Vibration and noise characteristics of the heavy commercial duty brake system in the type of drum brake are studied by numerical and experimental approaches to analyze the brake squeals. Natural frequencies and mode shapes of drum and shoe which are in frictional contact are determined by using finite element model developed in ANSYS. Experimental modal tests are performed to validate the finite element model. The noise characteristics of the brake system are measured by performance dynamometer in different braking scenarios having four parameters which are acceleration rate, pressure, temperature, and friction coefficients. The results show that noise problem is related with the velocity of vehicle up to 20 km/h, braking pressure about 2-6 bar, and temperature between 50 °C and 150 °C.

The finite element results for natural frequencies of drum and shoe are obtained very closely in experimental modal tests. However, the finite element results for natural frequencies of brake assembly are found for static condition, but experimental modal tests are performed in dynamical conditions due to the braking.

Sound measurements shows that the maximum noises are generated for $P_{max}$=6 bar for BS2 and BS4.

# REFERENCES


Ahmed, I., Allam, E., Khalil, M., and Abouel-seoud, S. 2012, Automotive Drum Brake Squeal Analysis Using Complex Eigenvalue, *International Journal of Modern Engineering Research*: 179-199.

Day, A.J., and Kim, S.Y. 1996, Noise and vibration analysis of an S-cam drum brake, *IMechE*: 35-43.

Disensors, 2010 http://www.disensors.com/downloads/products/7120A%20IEPE%20Accelerometer_1058.pdf

Gemeasurement, 2014 https://www.gemeasurement.com/sites/gemc.dev/files/unik_5000_datasheet_english.pdf

Glisovic, J., Radonjic, D., and Miloradovic, D. 2010, Experimental Method for Analyzing Friction Phenomenon Related to Drum Brake Squeal, *Tribology in industry*: 28-35.

He, J. and Fu, Z.F. 2001, Modal Analysis, Butterworth-Heinemann, Oxford.

Hussin, M.H., Bakar, A.R.H., Jamaluddin, M.R., and Szlapka, R., Effects of Lining Thickness on Squeal in Drum Brake Assembly: Experimental Investigations, *Int. J. Vehicle Structures & Systems*: 69-73.

Inman, D.J. 2006, Vibration with Control, John Wiley & Sons, West Sussex.

IMC, 2018, https://www.imc-berlin.de/produkte/messtechnik-hardware/imc-cronosflex/basiseinheiten/

IMC, 2018, https://www.imc-berlin.de/produkte/messtechnik-hardware/imc-cronosflex/messmodule/

Lee, J.M., Yoo, S.W., Kim, J.H., and Ahn, C.G. 2001, A STUDY ON THE SQUEAL OF A DRUM BRAKE WHICH HAS SHOES OF NON-UNIFORM CROSS-SECTION, *Journal of Sound and vibration*: 789-808.

Makeitfrom, 2009, https://www.makeitfrom.com/material-properties/Grey-Cast-Iron

MatWeb, 2011, http://www.matweb.com/search/datasheet.aspx?bassnum=MS0001&ckck=1

Nishiwaki, M., 1993, Generalized theory of brake noise, *ImechE*: 195-202.

Okamura, H., and Nishiwaki, M. 1989, A Study on Brake Noise, *JSME International Journal*: 206-214.

Phatak, A., and Kulkami, P. 2017, Drum Brake Backplate Analysis And Design Modification to Control Squeal Noise, *IJEDR*: 2321-9939.

Somnay, R., and Shih, S. 2002, Predicting Drum Brake Noise Using Finite Element Methods, ***SAE*** *Technical Paper Series*: 2002-01-3139.

Spurr, R.T. 1961, A Theory of brake squeal, *Proc Instn Mech Engrs*: 33-52.

Teoh, C.Y., Ripin, Z.M., and Hamid, M.N.A. 2013, Analysis of friction excited vibration of drum brake squeal, *International Journal of Mechanical Sciences*: 59–69.

Yardimoglu, B. 2015. Lecture notes on Finite Element Method, Izmir: Izmir Institute of Technology.

Yardimoglu, B. 2016. Lecture notes on Advanced Mechanics of Materials, Izmir: Izmir Institute of Technology.

Zhou, M., Wang, Y. and Huang, Q. 2007, Study on the stability of drum brake non-linear low frequency vibration model, *Arch Appl Mech*: 473–483.